AD-A109 908 PHILIPS LABS BRIARCLIFF MANOR NY F/G 13/1
DESIGN STUDY OF SMALL EFFICIENT CRYOCOOLERS.(U)
NOV 80 A SERENY, A DANIELS N00014-80-C-0464
UNCLASSIFIED NL

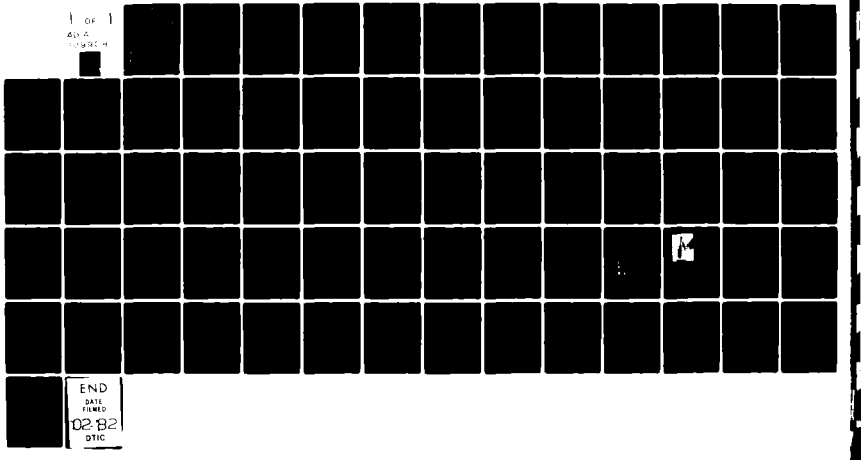

END
DATE FILMED
02-82
DTIC

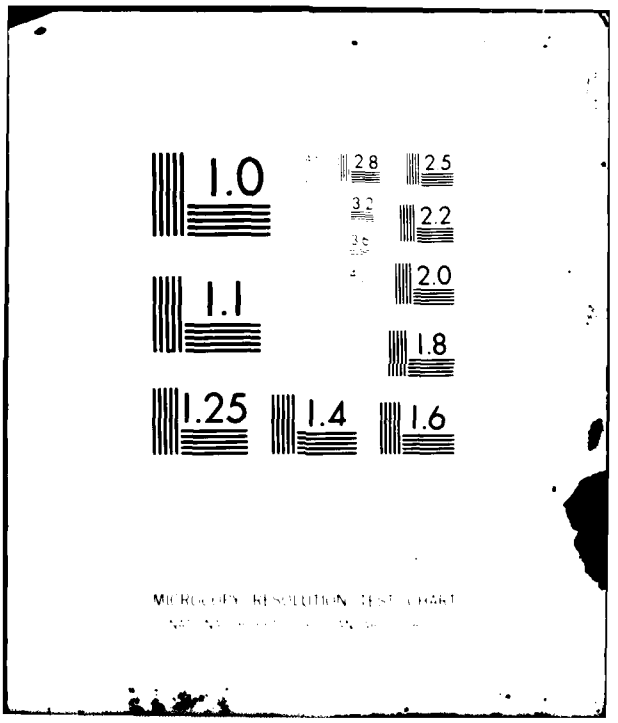
1.0
2.8
2.5
3.2
2.2
3.6
4
2.0
1.1
1.8
1.25
1.4
1.6

(4) cab

DESIGN STUDY OF SMALL EFFICIENT CRYOCOOLERS

PHILIPS LABORATORIES
A Division of North American Philips Corporation
Briarcliff Manor, New York 10510

November 1980

Final Report for Period 14 April - 11 September 1980

OFFICE OF NAVAL RESEARCH
Department of the Navy
Arlington, Virginia 22217

UNCLASSIFIED

SECURITY CLASSIFICATION OF THIS PAGE *(When Data Entered)*

REPORT DOCUMENTATION PAGE		READ INSTRUCTIONS BEFORE COMPLETING FORM
1. REPORT NUMBER	2. GOVT ACCESSION NO. AD-A104 988	3. RECIPIENT'S CATALOG NUMBER
4. TITLE *(and Subtitle)* DESIGN STUDY OF SMALL EFFICIENT CRYOCOOLERS		5. TYPE OF REPORT & PERIOD COVERED Final Technical Report April 14 - Sept. 11, 1980
		6. PERFORMING ORG. REPORT NUMBER
7. AUTHOR(s) A. Sereny A. Daniels		8. CONTRACT OR GRANT NUMBER(s) N00014-80-C-0464
9. PERFORMING ORGANIZATION NAME AND ADDRESS PHILIPS LABORATORIES A Division of North American Philips Corp. Briarcliff Manor, New York 10510		10. PROGRAM ELEMENT, PROJECT, TASK AREA & WORK UNIT NUMBERS
11. CONTROLLING OFFICE NAME AND ADDRESS OFFICE OF NAVAL RESEARCH Department of the Navy Arlington, Virginia 22217		12. REPORT DATE November 1980
		13. NUMBER OF PAGES 74
14. MONITORING AGENCY NAME & ADDRESS*(if different from Controlling Office)*		15. SECURITY CLASS. *(of this report)* UNCLASSIFIED
		15a. DECLASSIFICATION/DOWNGRADING SCHEDULE

16. DISTRIBUTION STATEMENT *(of this Report)*

Approved for public release: Distribution unlimited

17. DISTRIBUTION STATEMENT *(of the abstract entered in Block 20, if different from Report)*

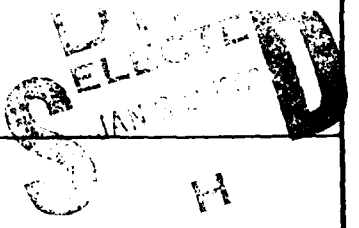

18. SUPPLEMENTARY NOTES

19. KEY WORDS *(Continue on reverse side if necessary and identify by block number)*

Stirling cycle refrigerator
cryogenic refrigerator for 10°K
triple-expansion Stirling-cycle refrigerator
free-displacer, free-piston system
cryocooler for superconducting elements
linear motor

20. ABSTRACT *(Continue on reverse side if necessary and identify by block number)*

A triple-expansion Stirling-cycle refrigerator driven by a linear mechanism was the configuration selected to best meet the requirements of this Phase I design study for a small, low-power, light-weight, efficient, closed-cycle cryocooler. The specifications for the cooling of superconductive magnetometers require the cryogenic refrigerator to operate at 10°K or less with a heat load of 50 mW, have an electrical input power not exceeding 250 W, and have minimum mechanical motion and magnetic signatures. The results of this

-Continued-

DD FORM 1 JAN 73 1473 EDITION OF 1 NOV 65 IS OBSOLETE

UNCLASSIFIED

SECURITY CLASSIFICATION OF THIS PAGE *(When Data Entered)*

20. ABSTRACT (Continued)

design study indicate that the 50 mW of refrigeration at 10°K with a maximum power input of 250 W can be readily met with a free-displacer, free-piston system. Three problem areas were identified and analyzed, viz., the lead regenerator matrix, piston seals, and output-temperature fluctuations. An analysis was also made of the magnetic effects of mechanical motion. This report concludes with an outline of the proposed efforts for a Phase II program.

PREFACE

Several members of Philips Laboratories' professional staff made significant contributions to the efforts summarized in this report. Dr. Chi Keung analyzed the temperature variation problem and the magnitude of the radiation load on the cold finger. Mr. Wyatt Newman, in consultation with Dr. Paul Shapiro, investigated the magnetic signature problem. Mr. Bruno Smits, Chief Designer, prepared the layout drawing.

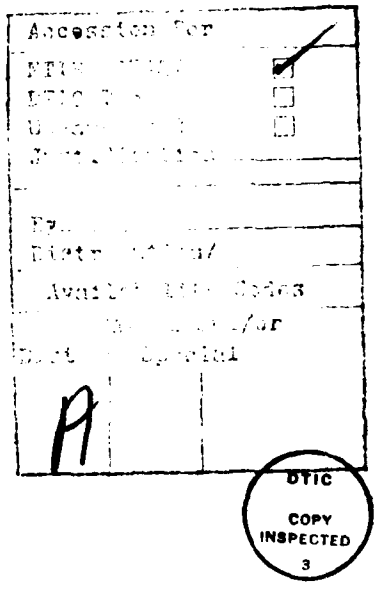

TABLE OF CONTENTS

LIST OF ILLUSTRATIONS

1. INTRODUCTION

Although their development is comparatively recent, super conductors have already been applied to power generation, computers, and metrology. Additional commercially promising applications, as well as their possible use in military systems, are currently being explored. However, to make superconductors more attractive to potential users, cryogenic refrigerators need to be developed that are capable of generating (efficiently and reliably) the required ultra-low temperatures.

One of the most promising superconductor applications is the detection of magnetic fields. However, it is this application where the need for a fieldable cryogenic refrigerator is perhaps the most acute, and where the superconductor/refrigerator interface is the most demanding. Under contract to the Office of Naval Research (ONR), Philips Laboratories studied the applicability of the Stirling refrigeration process to the cooling of magnetometers, and has generated a preliminary refrigerator design capable of meeting ONR's specifications.

The study had two major aspects: thermodynamic and interactive. The first addressed the thermal and physical characteristics of the refrigerator. The goal was to determine whether the cooling required by a magnetometer, specified as 50 mW at 10°K, can be generated by a refrigerator having an efficiency, weight, and size compatible with military applications, i.e., have relatively low power input, be comparatively light, and be small.

The second aspect of the study dealt with those facets of refrigerator design which are thought to affect the performance of the device to be cooled, viz., the magnetometer. The goal was to assess the nature of the magnetometer/refrigerator interface, i.e., the cold surface motion, the stability of the output temperature, and the magnitude of the magnetic fields generated by the refrigerator at its cold region. More specifically, the objective was to determine whether these factors would be compatible with the desired magnetometer output.

The thermodynamic aspects of the study had no significant uncertainties. Existing analytical tools, validated in laboratory prototypes and in commercially available hardware, were applied to a combination of proven concepts and novel approaches to yield design data which was then translated into a layout drawing. Specifically, the Philips Stirling Computer Program was used to optimize the critical parameters of a linearly driven, triple-expansion configuration. Where uncertainties did exist, the assumptions that had to be made were "conservative", to provide confidence that the performance predicted by the study could be attained in working hardware.

The interactive aspects of the study were less precise for three major reasons: the exact geometry and the physical characteristics of the magnetometer to be cooled were not inputs to the study; prior experience with, and current knowledge in, magnetic field generation in cryogenic hardware are not sufficient for rigorous quantitative work; and the magnitude of all three parameters of interest, i.e., vibrations, temperature variations, and induced magnetic fields, are subject to parametric trade-offs. Such a parametric study can best be done as part of the detailed design, i.e., in the next phase of the program. The nature of that phase of the program was the last item addressed by the study.

This report outlines the results of Philips Laboratories' analysis.

2. TECHNICAL DISCUSSION

2.1 Design Concept

A Stirling refrigerator generates cold by periodically expanding and compressing an ideal gas. The expansion takes place at the desired low temperature. The compression is maintained at ambient temperature with the aid of an external coolant. The working gas is usually helium.

The expansion and compression of the helium is accomplished by the reciprocating motion of a piston, complemented by the out-of-phase reciprocation of a displacer. The latter, as its designation implies, displaces gas from the cold region to the ambient temperature region of the machine (and vice versa) through a thermal regenerator.

The efficiency of a Stirling refrigerator depends to a very large extent on the manner in which the required expansion, compression, and regeneration is accomplished. For the ONR application, Philips Laboratories selected a triple-expansion configuration which has three expansion stages and three associated regenerators. The three expansions are produced by a single displacer (having three steps) which contains the three regenerators.

The efficiency of a cryogenic refrigerator also depends on the effectiveness with which the compression heat is dissipated. In the proposed design, that heat will be transferred to a liquid coolant in a counterflow heat exchanger. The proposed heat-dissipation method has been used often in the past.

The physical and operational chracteristic of a Stirling refrigerator, viz., it's size, weight, endurance, and reliability, depend to a large extent on the manner in which the piston and displacer are driven. The proposed design uses a linear drive in which there is no need to translate rotary motion into rectilinear motion. Because its motion is purely linear, the

proposed drive requires no bearings. Also, the seals on the piston and displacer are not subjected to the side forces normally present in a rotary/ linear drive approach.

A critical requirement in the application at hand is that the refrigerator/magnetometer interface be thermally efficient. The most difficult aspect of this interface is the motion (or vibration) of the cold surface, induced by the out-of-phase reciprocation of the moving masses. To eliminate such motion, or reduce it to a negligible level, the proposed refrigerator design will be passively balanced by a mass equivalent to, and moving in opposition to, the piston/displacer combination.

Many features of the proposed design, such as the triple-expansion configuration, the linear drive, and the balancing approach, have been demonstrated in operational hardware. The characteristics of these features are discussed in detail in the three sections which follow. Two other items, however, the coldest regenerator and the piston seal, although operationally demonstrated in the past, are thought to have a significant influence on the reliability of the proposed design, and are therefore discussed in a section devoted to the critical aspects of that design.

2.1.1 Triple-Expansion Configuration

To generate the required 50 mW of refrigeration at 10°K with a relatively high efficiency, the proposed design is a triple-expansion configuration. A detailed description of multiple expansion configurations is given in Appendix A; Philips Laboratories' specific experience with triple-expansion designs is also presented in this appendix. In principle, the triple-expansion process can be extrapolated one step further (i.e., to four expansions) to attain temperatures below 8.5°K, a possible future requirement.

Figure 1 depicts the proposed triple-expansion approach by showing a cross-section of the cold side, i.e., the combination of cold-finger (schematically), displacer, and three (3) regenerators. The cold finger is shown in greater detail in the layout drawing of Par. 2.1.5. The manner in which the displacer is integrated into the rest of the refrigerator is shown on that same drawing.

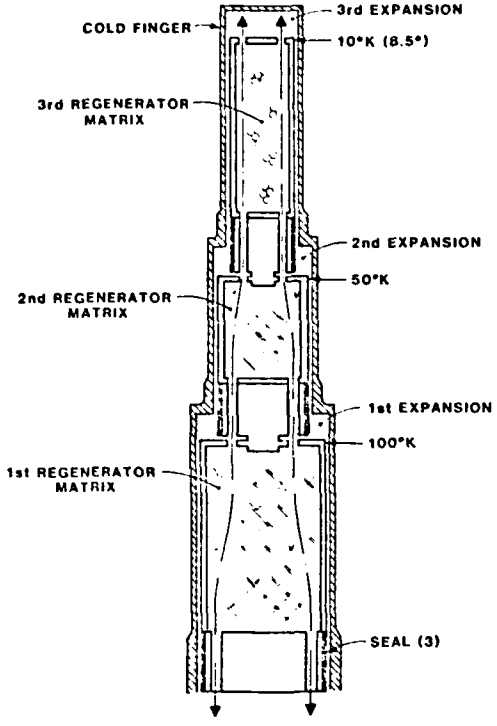

Figure 1. Proposed triple-expansion configuration.

As the arrows in Figure 1 indicate, the helium working gas flows from the compression to the expansion space (and back) through three regenerator matrices. At three points on this path, the gas is expanded. It is during these expansion processes that refrigeration is produced.

The first (warmest) regenerator matrix is made of phosphor bronze mesh with a filling factor of 30%. It is 31 mm in diameter by 49 mm long. Its cold end temperature is 100°K.

The second (intermediate) regenerator matrix is also made of phosphor bronze, but with a filling factor of 42%. It is 21 mm in diameter by 27 mm long. Its cold end temperature is 50°K.

The third and coldest regenerator matrix is made of lead spheres which are 140 μm in diameter. The matrix is 14 mm in diameter by 46 mm long. Packed spheres (of any size) yield a 63% (nominal) filling factor. The configuration of the lead (i.e., whether spheres or another geometry) in the matrix is critical to the life and reliability of the refrigerator. This aspect of low temperature regeneration is discussed in detail in Par. 2.2.1.

The helium working gas is prevented from flowing through the gap between the outside of the displacer and the cold finger, and thus from short-circuiting the regenerators, by the three sleeve-type seals shown in Figure 1. Seal effectiveness and endurance are discussed in Par. 2.2.2.

The analysis which led to the design shown in Figure 1 was based on the requirement for 50 mW (minimum) of refrigeration at 10°K, and zero refrigeration at 8.5°K. No net refrigeration is available at the intermediate temperatures (i.e., at 50°K and 100°K). However, these intermediate temperature levels could be used to cool radiation shields which would reduce the load on the coldest (i.e., 10°K) region. However, an accurate trade-off study of such a design can be rigorously addressed only when the geometry of the item(s) to be cooled is precisely known.

It should be noted that the displacer/regenerator subassembly reciprocates 500 times per minute at a maximum amplitude of 7 mm within the cold finger. Also, under the stresses imposed by the varying pressure in the refrigerator, the cold-finger wall strains cyclically. Both the intended and unintended motions (i.e., the displacer movement and the cold-finger strain, respectively) are expected to generate undesirable magnetic fields, as discussed in Par. 2.3.

In summary, the combination of the cold-side geometry depicted in Figure 1 and the matrix materials selected for the three regenerators is expected to produce the required refrigeration at the specified temperatures. However, the nature of the lead matrix and the choice of cold-side structural materials require further study, as discussed in Pars. 2.2.1 and 2.3.

2.1.2 Linear Drive

To impart the required rectilinear motion to the piston and displacer, the proposed design uses a purely linear drive, i.e., one devoid of rotary-to-linear conversion. The first such drive was designed at the Philips Research Laboratories in Eindhoven, The Netherlands, and applied to a Stirling refrigerator (designated Model MC-80) which produces 1 W of cold at 77°K. Currently, several linearly driven refrigerators with linear drive configurations are being developed within Philips, including two at Philips Laboratories in Briarcliff Manor.

A linearly driven refrigerator is often referred to as having a free displacer. *Indeed, the displacer is actuated by the* pressure difference created as a result of the flow losses through the regenerator (rather than mechanically). The gas flow is, of course, induced by the motion of the piston which is driven by a linear electric motor.

A schematic drawing of the proposed linear electromagnetic drive system is given in Figure 2. The major element of the system, viz., the motor, consists of a moving coil which is directly

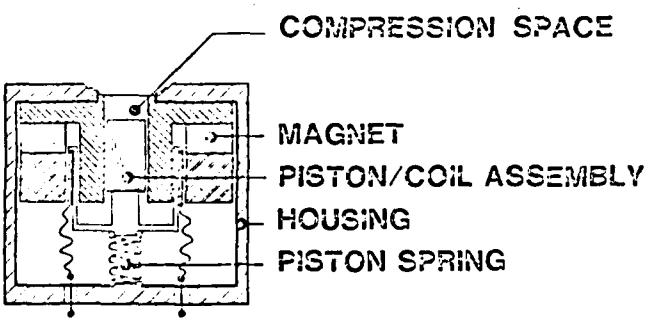

Figure 2. Linear electromagnetic drive.

coupled to the piston and free to reciprocate in a gap formed by a stationary permanent magnet and an iron yoke assembly. In such a configuration the gap length to gap width ratio is large, which permits a nearly uniform magnetic field to be established across the gap. Within that gap, a coil can reciprocate as the result of an applied ac current. The piston and linear motor are both sealed in a hermetic envelope, with the electric power transmitted through electric feedthroughs. The center position of the coil-piston assembly is held and controlled by a small mechanical spring.

It should be noted that linear motors can also be designed with moving magnets (rather than moving coils), in which case the need for flexing electrical leads is eliminated. However, moving-coil type motors are more efficient, a parameter of importance in this application. The motor proposed for this application has an efficiency of 70% at maximum amplitude. The flexing leads are not expected to affect the life and reliability of the proposed design; experience with the MC-80, as well as life test results with other units, suggests a flexing-lead endurance life considerably in excess of those expected in this application.

As indicated above, the displacer is "free", in as much as its motion is not mechanically imposed. To restrict its travel and to store energy as a means of enhancing refrigerator efficiency, the ambient temperature extremity of the displacer is anchored to the housing through a spring, as shown in the layout drawing given in Par. 2.1.5.

It should be noted that there is a significant difference between a conventional refrigerator drive and the linear approach proposed. In the former, the dynamics of the system are set by the parameters of the mechanical drive; therefore, the optimization of such a system deals with thermodynamic parameters only. In the linear approach, the dynamic parameters, such as the moving masses, have to be closely matched to

the thermal parameters of importance; therefore, optimization of the refrigerator is a thermodynamic/dynamic process, more difficult, of course, than the purely thermodynamic one. Some aspects of the thermodynamics and dynamics of the proposed linear approach are presented in Appendix B.

2.1.3 Passive Vibration Absorber

The use of a passive vibration absorber is proposed as a means for eliminating the refrigerator vibration at the fundamental frequency. A vibration damper in its most simple form consists of a mass connected to a spring which is connected to a machine for which attenuation of vibration is desired. The counter weight of a linear-drive Stirling refrigerator acts as a balancer for the combined sinusoidal motion of the piston and displacer. For a properly balanced system, the spring force produced by the reciprocating counter-weight will be just sufficient to nullify the forces upon the machine by the moving piston and displacer.

Philips has successfully applied passive vibration absorbers to cryogenic refrigerators and demonstrated a reduction of cold finger motion by nearly two orders of magnitude. Specifically, the MC-80 linearly driven refrigerator, using a balancing system similar to the one being proposed, has a cold side excursion in the range of 3 to 5 μm. It is probable that this range can be lowered with more sophisticated balancing techniques than those currently used.

2.1.4 Design Parameters

One of the major tasks of the study presented in this report was to determine the thermal and physical characteristics of a Stirling refrigerator design that can meet the requirements associated with the cooling of magnetometers (and other superconducting elements). Those requirements were specified in Section C of the ONR RFP No. N00014-80-R-0007 as follows:

- Operation at a temperature of 10°K (or less) for a heat load of 50 mW.
- Electrical input power not to exceed 250 W.
- Minimum mechanical motion and magnetic signatures.

In addition, reference was made to 8.5°K as the desired no-load temperature and to 4.2°K as a longer range goal for the operating temperature of small cryogenic refrigerators. Also, the variation in the operating temperature level was to be maintained within $\pm$ 0.01°K. The 250 W power input was a maximum, with 100 W (or less) as the goal. Finally, the refrigerator was to be small, light-weight, and reliable.

To meet the requirements outlined above, Philips Laboratories selected a triple-expansion, linearly driven, balanced design, as discussed in the previous paragraphs. Following that selection, an optimization study was conducted to arrive at refrigerator parameters (i.e., working pressure, operating frequency, piston and displacer strokes, regenerator dimensions, etc.) which would yield the best attainable efficiency, i.e., the lowest input power for the required refrigeration.

The analytical tools, i.e., the optimization program used in the study, had been validated through years of experience with operating hardware. However, it should be noted that designing a cryogenic refrigerator for very small cold outputs, such as the required 50 mW at 10°K, is an extremely sensitive process: a very small error, or unaccounted-for loss, can wipe out the desired net refrigeration. Therefore, to eliminate that danger, the design assumed a somewhat higher net refrigeration (0.1 W at 10°K). Thus, the results of the analysis are conservative.

The major refrigerator parameters that resulted from the optimization process are:

Number of expansion stages	3
Mean charge pressure	5×10^5 N/m^2
Working gas	helium
Operating speed	500 cpm
Drive system	free displacer linear drive
Type of linear motor	moving coil, stationary SmCo magnets
Piston amplitude and dia.	43.0 mm; 45.0 mm
Displacer amplitude	7.0 mm
Displacer diameters	14.3, 21.7, 31.6 mm
Mass of piston and moving coil	3.0 kg
Displacer mass	0.3 kg
Displacer spring stiffness	8500 N/m
Linear motor efficiency	70%
Counter weight	passive spring mass system
Maximum cold production	0.1 W at 10°K
Maximum power input	200 W electric
Cooler weight	74 kg
Cooler size	630 mm long, 350 mm diam (max)

Two items are to be noted. The parameters listed above are subject to trade-offs; for instance, efficiency (or power input) can be traded off for weight (and size). Such a study can be conducted in the next phase of the program in order to arrive at an "optimum combination" of parameters, rather than just optimum efficiency. Also, should the performance evaluation of the hardware indicate that the design was conservative, changes could then be made which would reduce the currently predicted 200 W input power level and the size and weight of the cooler.

2.1.5 Design Layout

The data that resulted from the analytical studies described in the previous paragraph was translated into the preliminary design depicted in the layout drawing of Figure 3. The drawing contains all the elements of the proposed refrigerator, except

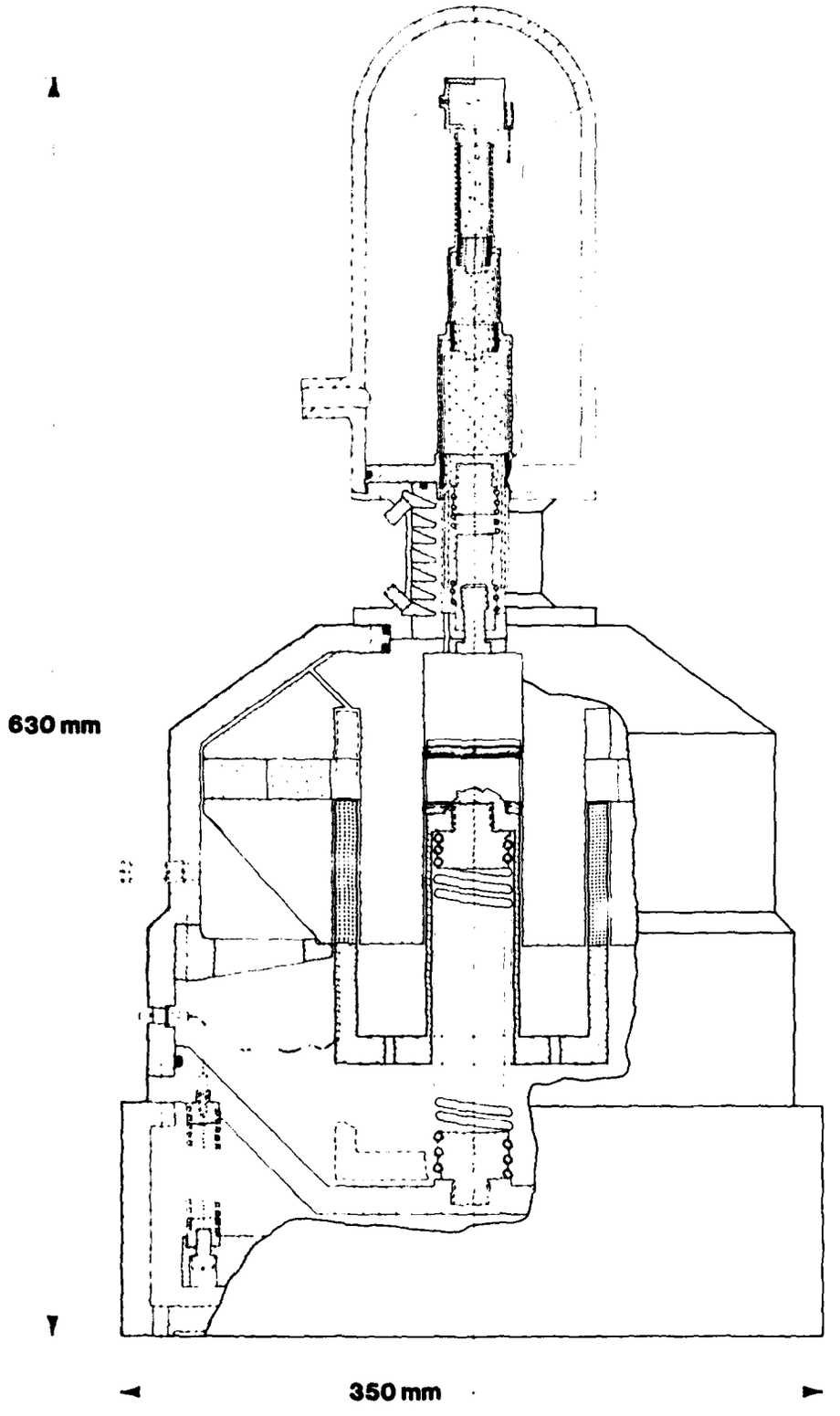

Figure 3. Layout drawing of proposed refrigerator.

those items which are normally designed or selected during the detailing phase.

The major features of the cold side are discussed in Par. 2.1.1. In addition to those features, the layout drawing addresses the methods for measuring the thermal performance of the refrigerator. Specifically, the layout shows a cavity at the cold end, which is to serve as the bulk of a gas thermometer, the most accurate means of measuring the lowest operating temperature. The capillary shown as penetrating the cavity wall would connect the thermometer bulb to an external pressure indicator. For redundancy, provisions were made to incorporate a platinum resistance thermometer into the cold region; the well shown next to the gas thermometer cavity would house the platinum resistor.

The chamber that surrounds the cold finger is a vacuum dewar to provide means of maintaining a pressure level below 10^{-4} Torr in that region, and hence to thermally insulate the cold finger. It should be noted that the geometry of the cold finger/vacuum dewar combination can be readily modified to accommodate a magnetometer or another superconducting element.

The "neck" that couples the cold finger to the body of the refrigerator is the ambient heat exchanger. Tubulations are provided for the inlet and outlet of the cooling medium.

The piston/linear motor combination, discussed in Par. 2.1.2, is enclosed in a hermetic housing. The only penetrations through that housing are the helium fill valve and the electrical feedthroughs for bringing power to the motor. The material of the housing will be either aluminum or titanium; the selection would be made in the next phase of the program.

The proposed refrigerator is 630 mm long, and the diameter at the largest cross-section is 350 mm. The weight breakdown is as follows:

Housing (assumed aluminum)	15.0 kg
Motor (perm. magnet and iron)	35.0 kg
Piston assembly	3.0 kg
Counterweight	15.0 kg
Displacer	0.3 kg
Cold finger	1.2 kg
Heat Exchanger	4.5 kg
Total	74.0 kg

The layout drawing of Figure 3 would provide the basis for generating the detailed design during the next phase of the program.

2.2 Critical Areas

Philips Laboratories' experience with the triple-expansion Stirling unit which was designed, built, and tested in 1969-70 indicates that the performance predicted for the proposed refrigerator can be attained. However, experience with the same hardware, as well as with other cryogenic refrigerators, suggests three potential problem areas: the structural integrity of the lead matrix in the lowest temperature regenerator; reliability, especially the rapid wear of conventional piston seals; and the need to maintain temperature stability to $\pm$ 0.01°K.

These problem areas, including proposed solutions, are discussed in the three paragraphs which follow. Another problem area, that of magnetic signatures, is discussed in Par. 2.3.

2.2.1 Lead Regenerator Matrix

The proposed design is based on the assumption that the lowest temperature regenerator matrix will contain lead spheres. Philips Laboratories used lead spheres in its triple-expansion Stirling refrigerator, as well as in the triple-expansion Vuilleumier refrigerator developed under contract to the U.S. Air Force (Flight Dynamics Laboratory, Wright-Patterson Field). The latter unit was developed for possible spaceborne use; therefore, life and reliability were critical parameters. During endurance testing of the Vuilleumier refrigerator, difficulties were encountered with the lead sphere matrix. The Hughes Aircraft Company encountered similar problems during tests with a triple-expansion Vuilleumier refrigerator which also contained lead spheres in the lowest temperature regenerator matrix.

Specifically, the lead spheres disintegrated after being loaded into the housing and subjected to tests, and the resulting dust clogged other critical passages. Philips Laboratories conducted an investigation to determine the cause of the problem, and

concluded that the failure was initiated by excessive oxidation of the lead spheres (Hughes Aircraft reached a different conclusion). A subsequent change in processing and packing of the lead spheres resulted in a matrix endurance period of over 4000 hours.

Shortly after the problem was identified, Philips Laboratories proposed a solution to the lead matrix problem, namely the use of lead mesh rather than lead spheres. The solution was implemented, tested, and found effective. However, since lead mesh is a "special" material, and, unlike spheres, not available commercially, spheres would be less costly.

The endurance evaluation of lead spheres is continuing. If the results of the evaluation are positive, the lowest temperature regenerator of the proposed design would contain lead spheres. Otherwise, Philips Laboratories would recommend the use of mesh. Our tests have shown that the thermal performances of spheres and mesh are equivalent. Thus, the performance predictions for the proposed design apply in either case.

2.2.2 Piston Seal

The sealing effectiveness and endurance characteristics of the piston seal are critical to the efficiency and reliability of the proposed (as well as any other) refrigerator design. Most commercially available cryogenic refrigerators use expansion-type (i.e., spring-loaded) rings to seal the piston. Those rings have acceptable sealing ability, but are subject to rapid wear. Other refrigerator designs, notably those being developed for possible spaceborne applications, propose the use of clearance-type seals which rely on a very small gap between the surfaces to be sealed to prevent gas leakage under dynamic conditions. Clearance seals are, of course, not subject to wear since there is no contact between the adjoining surfaces, but their sealing effectiveness is lower than that of expansion seals.

Unlike most other refrigerators, the piston of the proposed design is not subjected to lateral thrust; the lack of such thrust is conducive to very low wear rates, even when conventional seals are used. For the application at hand, however, Philips Laboratories proposes to use a novel seal design having very favorable endurance and sealing characteristics. The performance of the proposed seal was verified by testing.

The rate of wear of a piston ring depends on the product of its surface pressure exerted against the mating cylinder wall, and on its linear speed. For best performance, it is desirable to have the sealing ring gas-pressure-balanced, so that it is not pressed against the wall by the pressure wave variation. Also, the ring should be free-floating radially, so that the inaccuracies in the sideways guidance of the piston by the linear motor are not transmitted to the ring and thus cause it to wear.

The proposed piston seal design, described with the aid of Figure 4, incorporates both of the above features. A reinforced Teflon sleeve is fastened to the free-floating piston body and

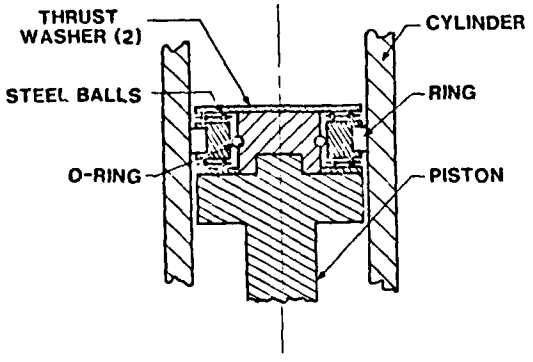

Figure 4. Piston seal design.

is machined to a sliding fit with the cylinder. At each end of this body are hardened steel balls backed up by hardened thrust washers. The balls have no lubrication and carry the gas pressure forces; they allow the thrust washers to move radially with the piston without transferring a side force to the ring

body. A phenolic separator plate is used as the ball spacer. A seal is made between the ring body I.D. and the piston, using a silicon rubber O-ring that is initially compressed more than the expected side motion of the piston. The relatively low pressure wave of the proposed refrigerator design is easily handled by this soft O-ring material, yet minimal side force is transmitted to the floating ring body. Since the ring body is a rigid member, it is inherently pressure balanced.

Because of this pressure balance and the free-floating features, ring wear is minimal. Calculations show that this type of ring will wear less than 0.025 mm radially in ten years. This minimal wear is due to the bearing friction induced by gas-pressure thrust and to the O-ring radial load imposed by the piston motion.

The proposed piston-ring design was tested in a double-expansion refrigerator for 1000 hours. At the end of this period there was no measurable wear or visual evidence of it (i.e., wear particles). Also, there was no phase shift in the refrigerator, an indication that there was no leakage past the piston seal.

2.2.3 Output Temperature Fluctuation

(1) Introduction

As a result of the nearly harmonic time variation of both the pressure and volume of the expansion space, the cold production in a Stirling refrigerator fluctuates about a mean value with time. This in turn gives rise to a fluctuating temperature at the cold end. An analysis was conducted to determine what parameters influence this fluctuation, what the magnitude of the temperature fluctuation in the proposed design are, and how the specified $\pm$ 0.01°K tolerance could be attained.

(2) Rate of Heat Transfer at Wall of Expansion Space

The helium gas in the expansion space is subjected to cooling or heating during the thermodynamic cycle. The rate of cooling or heating is equal to the expansion or compression work done on the gas by the motion of the displacer and piston. The wall of the expansion space is in turn cooled or heated by the helium gas. Due to the small heat capacity and high turbulent mixing of the helium gas in the expansion space, it is a conservative approximation (resulting in a higher temperature fluctuation) to equate directly the rate of cooling or heating of the wall to the work done by the displacer and the piston. This results in the following heat transfer rate Q at the wall:

$$Q = - p \frac{dV}{dt}$$

with $$p = p_m (1 - 2e \cos (\omega t - \theta))$$

and $$V = \frac{1}{2} V_o (1 + \cos \omega t)$$

$$Q = - p_m [1 - 2e\cos(\omega t - \theta)] [- \frac{\omega V_o}{2} \sin\omega t]$$

This can be written as

$$Q = -\frac{1}{2} p_m V_o \omega e \sin\theta - \frac{p_m V_o \omega}{2} \left[e\cos\theta \sin 2\omega t - e\sin\theta \cos 2\omega t - \sin\omega t\right] \qquad (1)$$

If the first and second term of the left-hand side of Equation (1) are denoted by Q_m and ΔQ, respectively, Equation (1) can be written as

$$Q = Q_m + \Delta Q$$

where, Q_m = time-averaged heat transfer rate and ΔQ = fluctuation in the heat transfer rate. Since $e << 1$, ΔQ can be approximated by:

$$\Delta Q = \frac{p_m V_o \omega}{2} \sin\omega t \qquad (2)$$

The effects of the other terms in ΔQ can be included by superposition of the results of the following analysis.

(3) Mathematical Modeling of Thermal Behavior of Wall

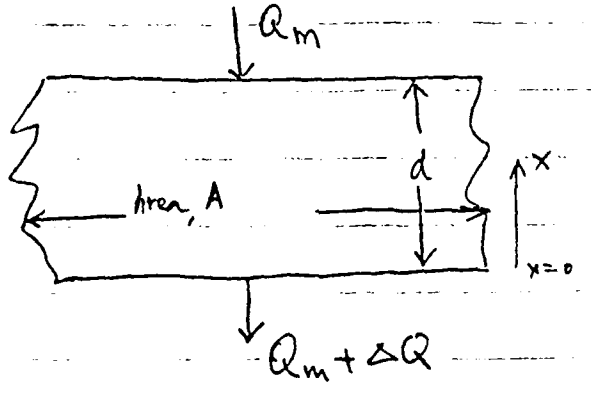

For steady state operation, the cooling load on the outside surface of the wall is Q_m, and the heat transfer rate on the inside surface of the wall is $Q_m + \Delta Q$. The boundary-value problem for the temperature is:

$$\rho c_p \frac{\partial T}{\partial t} = k \frac{\partial^2 T}{\partial x^2} \qquad 0 > x > d$$

$$+ k \frac{\partial T}{\partial x} = - \frac{1}{A} (Q_m + \Delta Q) \qquad \text{at } x = 0$$

$$k \frac{\partial T}{\partial x} = \frac{Q_m}{A} \qquad \text{at } x = d.$$

Let

$$U \equiv T + \frac{Q_m}{kA} x$$

The boundary-value problem can be rewritten as:

$$\rho c_p \frac{\partial U}{\partial t} = k \frac{\partial^2 U}{\partial x^2} \qquad 0 > x > d \qquad (3a)$$

$$k \frac{\partial U}{\partial x} = - \frac{\Delta Q}{A} = - \frac{p_m V_o \omega}{2A} \sin\omega t \qquad \text{at } x = 0 \qquad (3b)$$

$$\frac{\partial U}{\partial x} = 0 \qquad \text{at } x = d \qquad (3c)$$

For large values of d, the solution to this problem behaves like that of a semi-infinite body, and the steady periodic solution is:

$$U(x,t) = - \frac{p_m V_o \omega}{2Ak} \sqrt{\frac{\alpha}{\omega}} \; e^{- x\sqrt{\frac{\omega}{2\alpha}}} \sin\left(\omega t - \frac{1}{4}\pi - x\sqrt{\frac{\omega}{2\alpha}}\right) \qquad (4)$$

The depth at which the temperature fluctuation is damped to within 5% of the surface amplitude is, from Eq. (4),

$$x_{5\%} = 4.24 \sqrt{\frac{\alpha}{\omega}}$$

Therefore, if $d \geq 4.24\sqrt{\alpha/\omega}$, Equation (4) is a close approximate solution to Equations 3a-3c.

The amplitude of fluctuation of temperature $\tilde{T}$ at x = d can be obtained from Equation (4) as:

$$\tilde{T} = \tilde{U} = \frac{p_m V_o \omega}{2Ak} \sqrt{\frac{\alpha}{\omega}} \; e^{- d\sqrt{\frac{\omega}{2\alpha}}} \qquad (5)$$

From which,

$$d = \frac{\ln\left[\frac{p_m V_o \omega}{2Ak} \sqrt{\frac{\alpha}{\omega}} \; \frac{1}{\tilde{T}}\right]}{\sqrt{\frac{\omega}{2\alpha}}} \qquad (6)$$

Equation (6) gives the minimum thickness of the wall through which the temperature fluctuation is damped to $\tilde{T}$.

It can be observed from Equation (5), for a given amplitude of ΔQ, i.e., $p_m \omega V_o/2$, $\tilde{T}$ decreases with higher values of ω and k and lower values of α. An effective wall material for the purpose of damping the temperature fluctuation should have high k and low α.

(4) Design Considerations

To produce cold with a temperature fluctuation not to exceed 0.01°K, therefore, enough thermal inertia has to be built in the tip of the cold finger. According to Equation (5), a tip made of material with high thermal conductivity k and low diffusivity α provides better temperature stability. At temperatures around 10°K, lead possesses the above desirable combination of thermal properties.

The wall thickness of the tip of the cold finger required to damp temperature fluctuations down to specified values are plotted in Figure 5. The total cold production Q_{TOTAL} of 1.94 W is considered. Since the net cold production (total cold production minus losses through the cylinder walls and displacer) is only a fraction of the total cold production, curves for lower values of cold productions are also plotted in Figure 5. The corresponding temperature drops across the wall thickness are shown in Figure 6. Figures 7 and 8 are the same as Figures 5 and 6 with a larger heat transfer area A. It can be seen that an increase in A not only significantly reduces the thickness required to achieve a certain temperature stability, but also reduces the temperature drop across the wall thickness.

With a designed cold production of 100 mW (approximately $Q_{1/20}$) at 10°K, a temperature stability of 0.01°K can be obtained by using a lead tip of 1 cm thickness and a heat transfer area with a diameter of 2.86 cm (twice the diameter of the expansion space of the 3rd stage). The temperature drop across this thickness is less than 0.1°K.

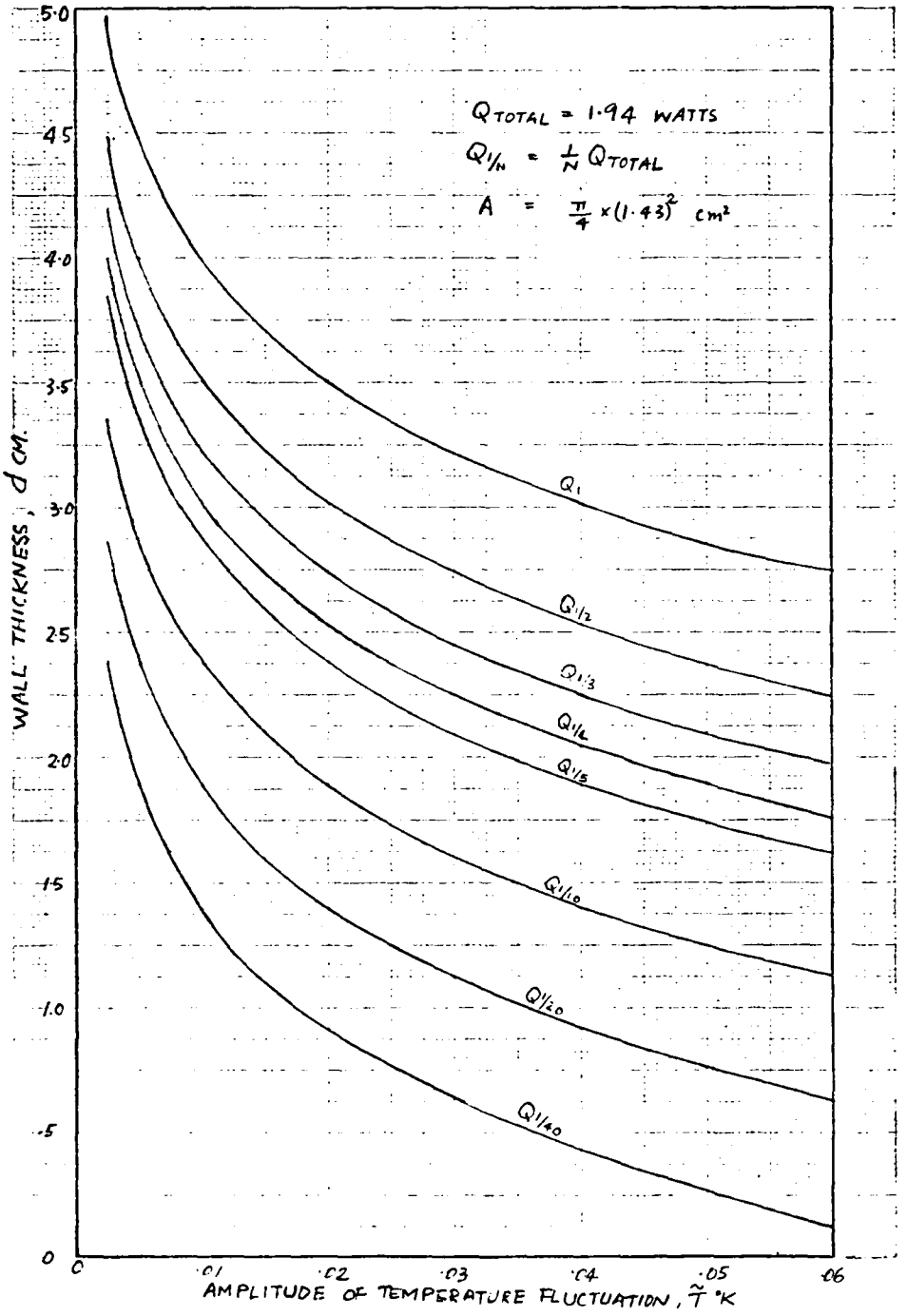

Figure 5. Wall thickness vs. amplitude of temperature fluctuation at various heat transfer rates (heat transfer area = 1.61 cm^2).

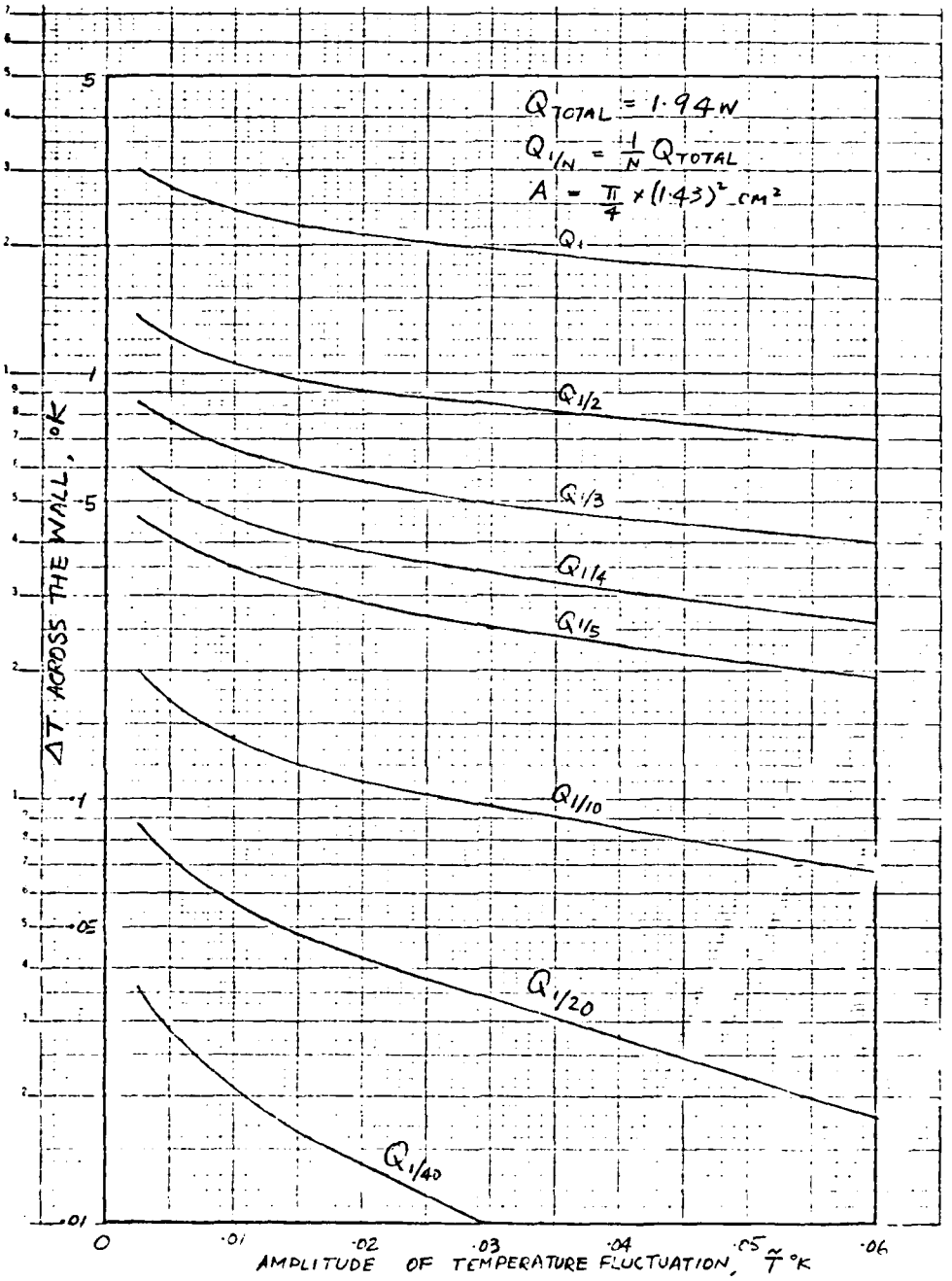

Figure 6. ΔT across wall vs. amplitude of temperature fluctuation at various heat transfer rates (heat transfer area = 1.61 cm^2).

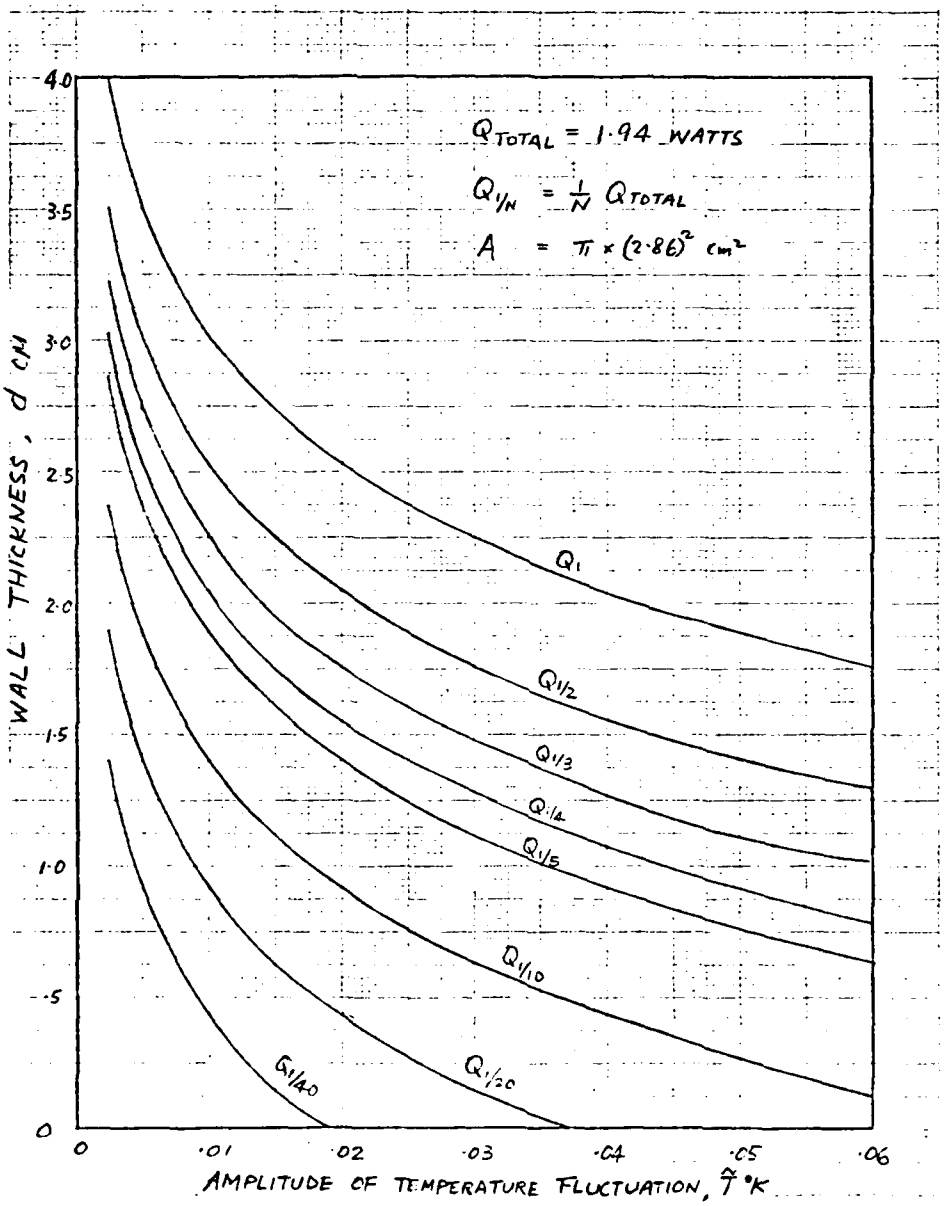

Figure 7. Wall thickness vs. amplitude of temperature fluctuation at various heat transfer rates (heat transfer area = 6.42 cm^2).

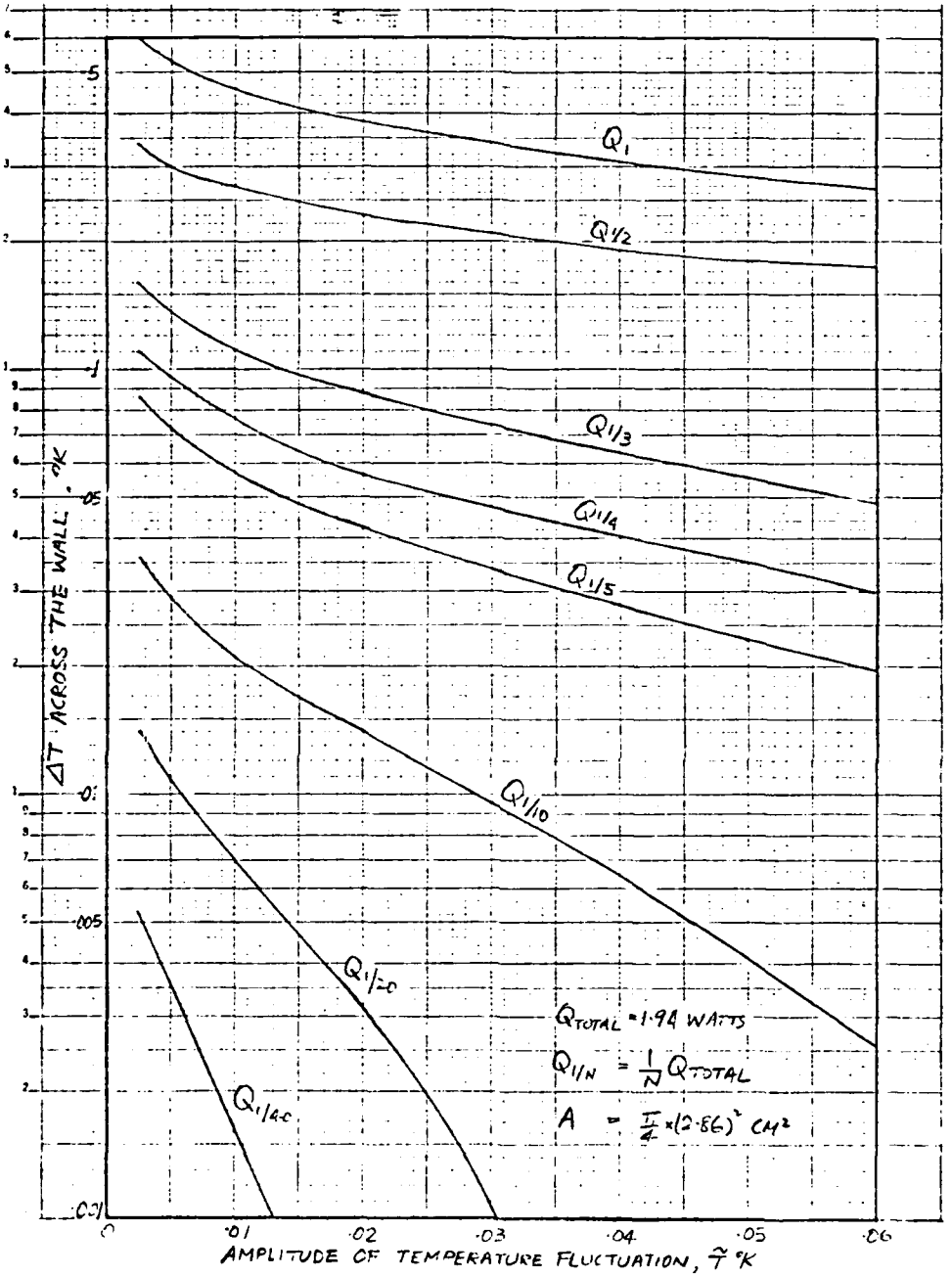

Figure 8. ΔT across wall vs. amplitude of temperature fluctuation at various heat transfer rates (heat transfer area = 6.42 cm^2).

In order to increase the heat transfer area A, the tip of a diameter larger than that of the expansion space can be used (Fig. 9). To ensure that the heat-flow process makes fuller use of the geometric cross-sectional area of the tip, a copper cap (higher conductivity than lead) can be added to spread out the path of heat flow (Fig. 9b).

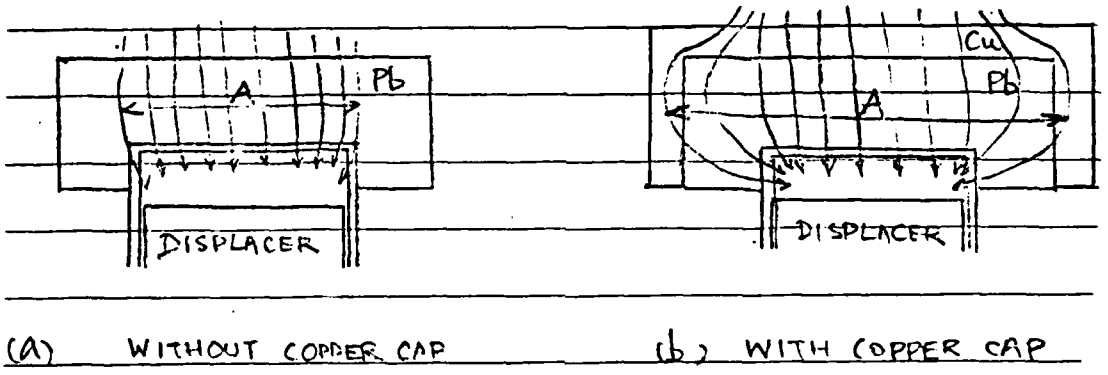

Figure 9. Schematic of heat-flow path in tip of cold finger.

(5) Conclusions

The specified ± 0.01°K output temperature tolerance can be attained by the interposition of a copper-sheathed lead mass between the expansion space of the refrigerator and the item to be cooled. Information was developed under this contract on the relationship of the attainable temperature fluctuation levels to other important parameters, such as temperature drop, cold production, and mass. The final selection of the optimum geometry, materials, mass, etc., of the method for attenuating temperature fluctuation can best be done during the next phase of the program, when information on the device to be cooled will be available.

2.3 Magnetic Effects of Mechanical Motion

The coupling of magnetometers (and other superconductive elements) to cryogenic refrigerators poses a difficult problem. Magnetometers are to be used in field applications for measuring very low frequency fields of 1 pT or less. Cryogenic refrigerators generate the required low temperatures by moving two masses, and that motion induces both vibrations at the cold end and strains in the adjoining walls. The vibrations and strains thus induced can give rise to magnetic fields higher than those that need to be detected. One of the most difficult challenges in the development of cryogenic refrigerators suitable for use in conjunction with superconductors will be to arrive at designs which will minimize, if not completely eliminate, the magnetic fields generated at the superconductor/refrigerator interface.

One of the factors which make the problem difficult is the lack of experience with this type of interface. The only significant work, to our knowledge, was done at the National Bureau of Standards by J.E. Zimmerman and his colleagues. However, it is obviously desirable to have an inertially balanced refrigerator design with a rigid (minimal strain) cold side structure. The balancing approach is discussed in Par. 2.1.3. The question of rigidity needs further elaboration.

Since electrical conductors moving in the earth's magnetic field generate eddy currents and unwanted magnetic fields, all cold side structural materials should be non-conductors, i.e., non-metals. Indeed, reinforced plastics have been used in the past for cold finger and displacer structures. However, the use of plastics in the working volume of a cryogenic refrigerator is undesirable since outgassing products contaminate the working fluid and contribute to performance deterioration. The proposed design was therefore based on the use of titanium at the cold end and lead and phosphorous bronze for the regenerators. To evaluate the field that would be generated by the titanium moving in the earth's field, a preliminary study, very general in its approach, was conducted.

As indicated, the motion of the electrically conducting components of the proposed refrigerator in the earth's magnetic field will produce magnetic interference. The conductors react to time-varying magnetic flux and to accelerations in the presence of a uniform magnetic field by generating eddy currents which produce reaction magnetic fields. Worst-case effects are modeled below, and estimates of magnetic interference are made for a miniature cryocooler design.

The first case to be considered is that of a pulsating cylindrical shell (the cold finger, for instance) in a uniform magnetic field. The pulsating shell models the strain of the expansion chamber enclosure induced by the internal pressure variations. For a pressure variation of the form

$$\Delta P(t) = \Delta P \sin \omega t,$$

a thin shell will respond by straining an amount:

$$\frac{\delta r(t)}{r} = \frac{r}{t} \frac{\Delta P(t)}{E}$$

where, t = shell thickness
r = radius
δr = change in radius
E = Young's modulus

Thus, the flux area normal to the axis varies as:

$$\frac{dA}{dt} = \frac{2\pi r^3 \omega \Delta P \cos \omega t}{tE} ,$$

and the peak magnetic flux change is thus:

$$\left|\frac{d\phi}{dt}\right|_{max} = \frac{2\pi r^3 \omega \Delta P}{tE} B_a$$

where B_a is the magnitude of the ambient magnetic field in the axial direction. The changing magnetic flux induces a circumferentially circulating current in the shell, which is inversely proportioned to the circuit resistance R. Since the reaction magnetic field is proportioned to the circulating current,

$$B_{reaction} \simeq \frac{\mu_o B_a r^2 \omega}{2\rho} \frac{\Delta P}{E}$$

where ρ = resistivity of shell

μ_o = magnetic permeability of free space.

The preceding estimates the peak field at one end of an axially semi-infinite solenoid formed by a thin shell. The semi-infinite solenoid approximation is conservative, since a shorter solenoid produces a weaker field. Also, the thin shell approximation is somewhat conservative, since the shell is actually constrained at the ends, which reduces the radial strain and thus reduces the flux area variation.

Parameters for estimating this effect for the cold finger of the proposed refrigerator are as follows:

$r \sim 1$ cm

$\Delta P \sim 2 \times 10^5$ N/m^2

$\omega \sim 20\ \pi$sec^{-1}

$\rho \sim 5 \times 10^{-8}$ Ω-m (for titanium at 10°K)

$E \sim 1 \times 10^{11}$ N/m^2 (for titanium at 10°K)

$B_a = B_e \sim 50$ μT for worst case operational orientation (horizontal in N-S direction)

Then, $B_{reaction} \sim 10$ pT.

A field of this magnitude is expected to present a problem for measurements in the pT range. However, the field could be

significantly reduced by: shielding, choice of operational orientation, choice of material with different ρ and E, and variations in design parameters of r, ω and ΔP.

The second case to be considered is that of a changing magnetic flux due to motion in a non-uniform field. In unshielded rooms, field gradients of 10 μT/M are not uncommon. This effect is estimated for the displacer, which is modelled as a cylindrical shell which oscillates in the axial direction, x, with amplitude a. The maximum flux variation occurs when motion is along the field gradient. The cases of field orientation parallel and normal to the axis of symmetry are considered separately below.

For the case of a field and a field gradient that are both axially aligned, the flux variation for the previously described cylindrical shell is:

$$\frac{d\phi}{dt} = \pi r^2 \frac{dB}{dt} \quad \text{and} \quad \left|\frac{dB}{dt}\right|_{max} \simeq \left|\frac{dB}{dX}\right| \left|\frac{dX}{dt}\right| = \frac{dB}{dX} a\omega$$

Applying the semi-infinite solenoid approximation as before yields the relation:

$$B_{reaction} \simeq \frac{\mu_o r a \omega t}{4\rho} \frac{dB}{dX}$$

For the same parameters as before, with a shell thickness t of 0.2 mm, an amplitude, a, of 6 mm, and a field gradient of 10 μT/M in the axial direction, the reaction field is:

$$B_r \sim 50 \text{ pT.}$$

The effect of the regenerator matrix within the oscillating shell is difficult to determine, since the electrical conductivity of the matrix could vary drastically. The matrix can be modelled as a set of concentric shells which behave as the shell analyzed above. The reaction field is then proportional to the effective matrix conductivity. The conductivity could be made

much lower than that of the outer titanium shell. As a rough upper bound, the regenerator may produce interference on the same order as that of the outer shell described above.

For the case of axial field gradient in a field normal to the axis, eddy currents will circulate about the field direction on the surface of the shell, as opposed to the circumferential currents of the first two cases. The cylinder observes the same magnitude of time varying magnetic field as the prior case, but the flux area is now the projection of the cylinder surface area. The result of integrating over concentric current loops is that peak reaction fields are roughly the same as those of the prior case with the same functional dependence on r, a, ω, t, ρ, and dB/dX.

The estimated reaction field is worst case since it assumes that no attempts have been made to reduce ambient field gradients, and that a strong gradient is aligned with the machine's axis. Also, the reaction could be reduced somewhat by varying design parameters.

The last effect to be estimated is that of the reaction field due to the acceleration of charges in a uniform magnetic field. An estimate can be made by considering a flat plate oscillating in the presence of a magnetic field, B_e. The plate considered oscillates normal to its surface. The magnetic field is directed parallel to the surface. The plate has dimensions "ℓ" by "ℓ" and it oscillates with amplitude "a" and angular frequency "ω". Conduction electrons in the plate experience forces normal to the velocity and to the field. This causes a nearly linear charge distribution on the plate, which changes as the velocity changes. Redistribution of charges results in currents in the plate which are proportional to the plate's acceleration. The resulting reaction magnetic field is proportional to the currents. The reaction field B_r is:

$$B_r \sim \mu_o \varepsilon_o \ell a \omega^2 B_e$$

where, ε_o = permittivity of free space and $a\omega^2$ = peak acceleration of the oscillating plate. Filling in constants and rough design parameters yields an immeasureable response of about 10^{-18} B_e, or about 10^{-22} T.

The preceding analysis suggests that the influence of induced eddy currents could be a problem. It appears that the estimated interference is reducible, possibly to acceptable levels. This preliminary estimate also suggests that magnetic noise could result from the operation of cryogenic refrigerators due to vibrations and rotations transmitted to the magnetic detector in the presence of the earth's field. Thus, the use of conductors as refrigerator components should not be ruled out, since structural rigidity and vibration compensation are likely to be of critical concern.

It should be noted that if further investigation of the titanium cold end indicate significant problems, the titanium can be replaced with a reinforced plastic; the major parameters of the design would not change significantly. The conduction losses would increase somewhat, and the unit would probably have to be purged periodically to "flush out" the contaminants.

It should also be noted that the regenerator matrices now reciprocating with the displacer could be made stationary. In such an approach, the matrices would be placed outside the displacer in an annular geometry. Such a design is associated with more dead space and with a more complex cold side construction.

The two alternative approaches just outlined, i.e., the use of plastics rather than titanium, and of stationary rather than moving regenerators, are practical, but thermally and structurally less attractive. A final choice can best be made as part of a rigorous trade-off study proposed for the next phase of the program.

2.4 Remarks

Following completion of the proposed design, an effort was made to compare its major features to those of other cryogenic refrigerators which operate at approximately the same temperature level. However, the only refrigerators which operate in the 8°K to 15°K range are very large units, with significantly higher cold producing capacities than the 50 mW output of the proposed design. Therefore, the comments which follow are qualitative rather than quantitative, reflecting the difficulty of a one-to-one comparison.

The proposed design is based on the Stirling cycle, which is thermodynamically reversible; hence, it has the highest attainable efficiency (ideally). Indeed, experience has shown that for small refrigeration requirements, no other cycle has been mechanized with higher efficiency. Our study suggests that the specified efficiency, i.e., 50 mW of refrigeration at 10°K with 250 W (maximum) power input, can be readily met. Furthermore, the 100 W ultimate goal appears to be realistic.

The proposed design is a "one-piece" configuration, rather than "split". The latter approach, whether based on the Stirling or the Gifford-McMahon cycle, has to contend with significant losses through the required connection between the expansion and compression spaces. The supposed advantage of a low-vibration expander of a split cycle is matched by the very low vibrations attainable with a balanced one-piece construction.

A significant advantage of the proposed design (versus split cycle approaches) is the lack of valves, which are associated with losses and present reliability problems.

It should be noted that the only possible disadvantage of the proposed system is its comparatively high weight, which is due to the nature of a slow-speed linear motor and the need for a balancing countermass.

3. OUTLINE OF PHASE II

3.1 Introduction

Philips Laboratories recommends that the design presented in this report be detailed during the next phase of the program. Those details would then be translated into working hardware during a subsequent phase. The proposed efforts would consist of five major tasks:

- Parametric trade-off study and review of current design.
- Preparation of manufacturing drawings.
- Review of material(s) availability.
- Preparation of a manufacturing schedule and a test plan.
- Report of Phase II results.

The suggested tasks are discussed in detail next.

3.2 Discussion of Proposed Program

(1) Parametric Study and Review

Prior to preparation of manufacturing drawings, efforts are recommended to:

- Refine the current design so that it reflects the Contracting Agency's priorities regarding refrigerator characteristics.

As indicated in this report, the Philips computer program, which mathematically formulates and interrelates the various design parameters of the Stirling cycle, would permit the selective optimization of the cycle's important characteristics. For instance, efficiency, normally an optimized parameter, can be traded-off for weight; life can be traded-off for weight; etc. Philips Laboratories recommends that before the layout drawing of Figure 3 is translated into details, a trade-off study be made to arrive at an optimum combination of important refrigerator characteristics.

Such a study rquires a priority listing of refrigerator characteristics, i.e., a ranking of efficiency, weight, size, life, reliability, etc. Based on such a listing, curves can be prepared showing the interrelationships of the various parameters. With the assistance and concurrence of the contracting agency, nominal design points would be selected from the parametric curves.

With the new values as a starting point, the current design would be reviewed and, most likely, minimal dimensional changes would be made. These changes would be incorporated in the layout drawing, which would then serve to initiate the next task, viz.,

- Make final choices where design options still exist.

As indicated in the report, many design choices are best made during the transition from the layout drawing to the manufacturing drawing. Areas which would require further consideration during the next phase include: the lead matrix in the coldest regenerator, the method of static sealing (whether with elastomeric or metal seal), and the material for the refrigerator envelope. Then,

- Expand current layout drawing to include all hardware details.

With the major design options finalized, the next task of the proposed program would include: selection of an assembly procedure, which requires that fastening methods be established; selection of motor manufacturing processes; and a stress analysis of the critical refrigerator components.

(2) Preparation of Manufacturing Drawings

Completion of the task outlined above would permit the initiation of the design detailing process. It should be noted that the detailing process includes close engineering monitoring to insure that the thermodynamic characteristics of

the refrigerator are not altered by design compromises. The end result of this task would be a drawing package from which an engineering prototype could be fabricated.

(3) Review of Material(s) Availability

There is a possibility that some of the materials to be included in the proposed refrigerator are not available "off-the-shelf". This condition normally leads to significant delays in the manufacturing process. To eliminate or ease that condition, it is recommended that parallel to the detailing process, efforts be conducted to identify long-lead materials, and to place purchase orders if warranted. This activity requires coordination with the contracting agency.

(4) Preparation of Manufacturing Schedule and Test Plan

This task is recommended as a means of facilitating the planning and conduct of the subsequent phase of the program. The preparation of a test plan can be especially effective in this respect, for it identifies provisions which have to be made in the hardware for accommodating instrumentation. Concurrently, of course, it identifies the required instrumentation and test facilities.

(5) Report

The fifth task would be the preparation of a report, which would include a description and discussion of the design developed during this phase, and detailed plans for the third phase of the program.

APPENDIX A

Expansion Staging for Regenerative Cycles

APPENDIX A

EXPANSION STAGING FOR REGENERATIVE CYCLES

Regenerative type refrigeration cycles, e.g., Vuilleumier (VM) and Stirling, produce cold by the reversible expansion of an ideal gas. The number of expansion stages and their geometry have a significant effect on the efficiency with which the required cold can be produced. The design aspects of single and multiple expansion refrigerators are discussed below.

1. Single Expansion

The characteristics of the VM and Stirling cycles are normally described by depicting one expansion space of the refrigerator (Ref. 1). The configuration of a typical VM or Stirling cycle "cold cylinder", i.e., expansion space, displacer, and regenerator, is shown in Figure 1. In principle, ideal regeneration

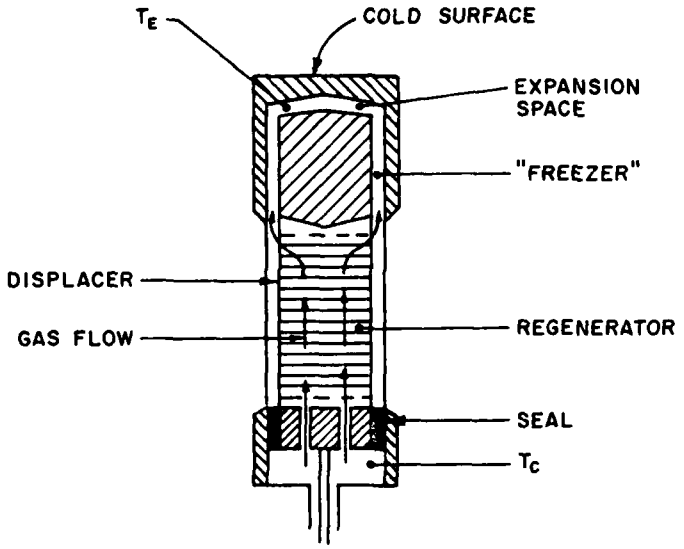

Figure 1: Typical Single Expansion Configuration

is possible in both cycles, since the same quantity of gas flows through the regenerator in both directions, with the same temperature difference, i.e., $T_C - T_E$. The amount of heat rejected and absorbed by the gas for both directions of flow is the same, since the specific heat for nearly perfect gases is essentially independent of pressure.

In actual practice, the regeneration is not ideal, i.e., there is a small departure from the ideal caused by imperfect heat transfer. In a typical regenerator, a quantity of heat Q_r must be absorbed and rejected during each cycle. Due to various imperfections, this amount is reduced to $\eta_r Q_r$, where η_r is the efficiency of the regenerator. This means of course that not all of the available heat is transferred to the regenerator. The rest, that is $(1-\eta_r)Q_r$, is carried along with the gas through the regenerator, so that the temperature of the gas flowing into the expansion space is somewhat above that desired. This remainder, which we will designate as ΔQ_r, constitutes the regeneration loss. Since this loss must be made up from the refrigeration produced Q_E, it should be compared with Q_E. Calculations show that:

$$\frac{\Delta Q_r}{Q_E} = C_r(1 - \eta_r) \frac{T_C - T_E}{T_E} \qquad (1)$$

The constant C_r depends mainly on the compression ratio in the refrigerator; for small units, its value is approximately 10. For example, if $T_C = 300°K$, $T_E = 75°K$, and the regeneration loss $1-\eta_r = 1\%$, we find:

$$\frac{\Delta Q_r}{Q_E} = 30\%$$

This means that a 1% loss in regeneration involves a 30% loss in refrigeration. It is therefore clear that for efficient operation, the regeneration loss in a VM or Stirling unit has to be minimized.

In practice, refrigerators having only a single expansion chamber are referred to as "single expansion" units.

2. Possible Improvements

Equation (1) for the relative regeneration loss suggests two possible methods for improving the refrigeration process: decreasing the value of C_r, and increasing the value of η_r.

The way to decrease C_r would be to increase the compression ratio since C_r depends mainly on this ratio. At present, no practical configurations exist to achieve this in either the VM or Stirling cycles.

The value of η_r, about 99% in typical regenerative refrigerators, can be increased somewhat. Regenerators with efficiencies of 99.5% and higher have been made. However, since a regenerator with such high efficiencies normally has very high flow losses, lower refrigerator efficiency will result.

3. Double Expansion

To avoid the disadvantages cited above, Philips, in 1963, modified the conventional single expansion system (Ref. 2). The modification consisted of thermally staging a number of expansion processes in as many expansion spaces. The method is somewhat analogous to the Keesom cascade process, except that no separate thermodynamic cycles are used, since the complete cycle is performed in one closed system. This modified cycle has been referred to as the "double expansion" cycle.

In this method the expansion is performed in two expansion spaces, each at a different temperature. The spaces are connected in series, with regenerators in the interconnecting passages. The displacer used in the single expansion machine has been adapted to the double expansion process, as shown in Figure 2. The additional, intermediate expansion space M_M is obtained by "stepping" the diameter of the displacer. By virtue of this stepped displacer, volume variations of the two expansion spaces (E and M) are in phase. The advantage of this type of construction is that the pressure difference across the seal between the expansion spaces is small, as in the conventional design.

As a result of the additional expansion space, the refrigerator produces cold at two different temperatures, whereas in the conventional process cold production takes place at only one temperature. The resultant advantages are discussed in Paragraph 4.

The following discussion shows how this system reduces the influence of the regeneration loss. Assume that a mass of

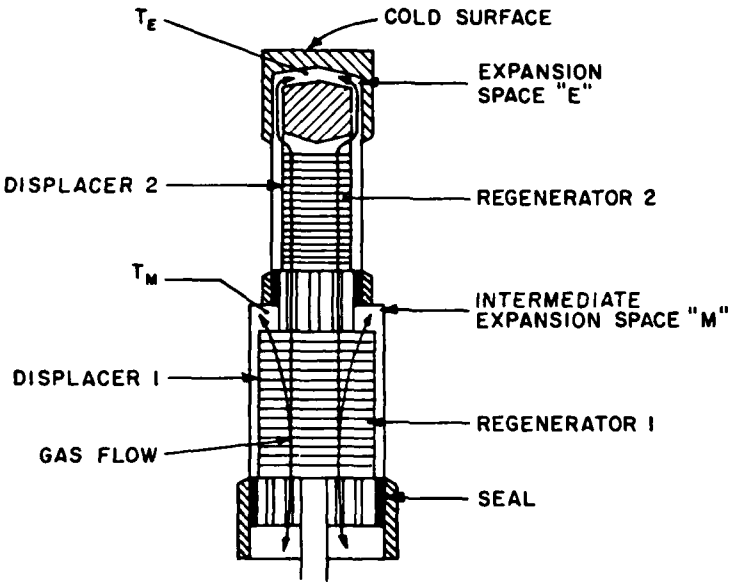

Figure 2: Typical double expansion configuration

working gas m_M is expanded in the intermediate expansion space at a temperature T_M, and that a mass of working gas m_E is expanded in the top expansion space at a temperature T_E - both gases expanding from a pressure p_1 to a pressure p_2. The ideal cold productions in the expansion spaces are:

$$Q_M = m_M R T_M \ln(p_1/p_2)$$

$$Q_E = m_E R T_E \ln(p_1/p_2)$$

The mass flowing through regenerator 1 between room temperature and the intermediate temperature now is $m_M + m_E$, and the mass flowing through regenerator 2 between the intermediate space and the expansion space is m_E. The regeneration losses for these regenerators are:

$$\Delta Q_{r1} = (m_M + m_E)\, C_p (1 - \eta_{r1})(T_C - T_M)$$

$$\Delta Q_{r2} = m_E C_p (1 - \eta_{r2})(T_M - T_E)$$

Hence, the relative regeneration losses are:

$$\frac{\Delta Q_{r1}}{Q_M} = \frac{m_M + m_E}{m_M} C_r (1 - \eta_{r1}) \left(\frac{T_C - T_M}{T_M}\right) \qquad (2)$$

$$\frac{\Delta Q_{r2}}{Q_E} = C_r (1 - \eta_{r2}) \left(\frac{T_M - T_E}{T_E}\right)$$

It should be noted that C_r again has the same value if P_1/P_2 has the same value, i.e., about 10.

Now $\Delta Q_{r2}/Q_E$ is small, because T_M is of the order of 140°K, and T_M-T_E is therefore less than T_C-T_E, the quantity that occurred in Equation (1). The consequence is that little of the cold production in the top expansion space is lost, thereby resulting in a relatively large increase in net cold production. When the refrigerator of interest needs cold at one level only, no net production Q_M is needed, and it is permissible for $\Delta Q_{r1}/Q_M$ to be of the order of unity. Taking the efficiency of regenerator 1 to be 98%, it follows from Equation (2) that:

$$\frac{\Delta Q_{r1}}{Q_M} = 0.2\, \frac{m_M + m_E}{m_M}$$

Hence, $(m_M + m_E)/m_M$ can have a value of about 5. This means that in a refrigerator using a double expansion configuration only a mass of about one-fifth of the total mass flowing through the first regenerator needs to be expanded in the intermediate space; this causes only a relatively small increase in the compression work.

4. Applications

It is evident from the foregoing that given the same conditions, i.e., cold production at a given operating temperature, the double expansion configuration is more efficient. There is, however, additional complexity, viz., two regenerators instead of one. It should be noted that an intermediate temperature level in the double expansion configuration offers significant advantages in some cases. For instance, in certain applications where radiation shielding is desirable, the shield can be cooled at the intermediate temperature level. The required refrigeration can of course be produced more efficiently at this level.

Both the single and double expansion configurations have been incorporated in many operational systems. Figure 3 shows, for comparison, single and double-expansion displacer-regenerators of a VM refrigerator producing 1 W at 77°K. The construction is similar in both cases.

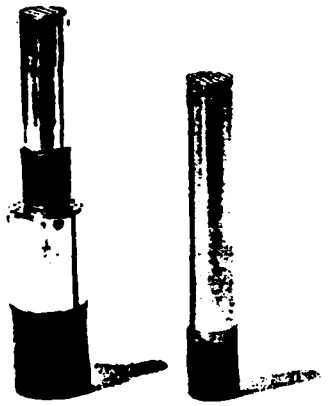

Figure 3: Single and double expansion displacer-regenerators of a VM refrigerator producing 1 W at 77°K.

The multi-expansion concept has been extended one step further to a triple-expansion Stirling cycle configuration (Ref. 3), as well as to a triple-expansion Vuilleumier refrigerator. In both cases, temperatures as low as 7.2°K, with only one cycle, have been attained (Ref. 4). Figure 4 shows the displacer-regenerators of the Vuilleumier refrigerator.

Figure 4: Displacer-regenerators of Vuilleumier refrigerator.

5. References

(1) A. Daniels, "Cryogenics for Electro-Optical Systems," Electro-Optical Systems Design, vol. 3, pp. 12-20, July 1971.

(2) G. Prast, "A Philips Gas Refrigerating Machine for 20°K," Cryogenics, vol. 3, pp. 156-160, September 1963.

(3) A. Daniels and F.K. du Pré, "Triple-Expansion Stirling Cycle Refrigerator," Advances in Cryogenic Engineering, vol. 16, pp. 178-184, June 1970.

(4) G.K. Pitcher, "Development of Spacecraft Vuilleumier Cryogenic Refrigerators," AFFDL TR-71-147, Part I, Contract F33615-61-C-1024, December 1971.

APPENDIX B

Dynamics of a Free-Displacer, Free-Piston Stirling Refrigerator

APPENDIX B

Dynamics of a Free-Displacer, Free-Piston Stirling Refrigerator

1. INTRODUCTION

The Stirling cycle is characterized by the interphased reciprocating motion of its two major elements, the piston and the displacer. Traditionally, this motion was generated by either conventional crank-type mechanisms or by the Philips rhombic drive. In both instances, the rotary motion supplied by an electric motor had to be translated into the required rectilinear motion of the piston and the displacer.

In the early 1970's, the Philips Research Laboratory of Eindhoven, The Netherlands, designed a Stirling cryogenic refrigeration system in which the piston was reciprocated by a linear electric motor; the piston in turn, by fluidic force coupling, drove (linearly) the displacer. The novel approach eliminated the need to translate rotary to linear motion.

The new refrigerator, currently in industrial and military use, offers constructional simplicity, and hence high reliability. Its major characteristics are described in the following section as an aid in understanding the design presented in this report.

2. DESCRIPTION

A simplified cross section of the refrigerator is shown in Figure 1. The low temperature (or expansion) side contains the displacer which contains the thermal regenerator. The ambient-temperature (or compression) side contains the piston which is directly coupled to the moving coil of the permanent-magnet-type linear motor.

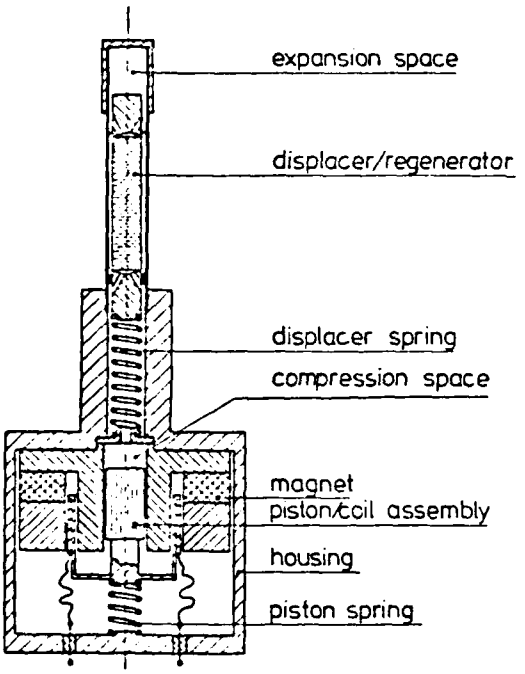

Fig. 1. - Schematic cross section of linear refrigerator.

The permanent magnet maintains an approximately constant field in the gap which surrounds the inner iron yoke of the motor. The coil, activated by an AC current, reciprocates in the gap, imparting the required linear motion to the piston. A spring attached to the outer extremity of the piston/coil subassembly defines the center position of the piston.

The displacer is driven by the pressure differential established by the losses of the helium working gas as it flows back and forth through the regenerator matrix. A spring attached to the ambient temperature extremity of the displacer insures proper phase relationship between the moving masses.

It should be noted that all the forces acting on the piston and displacer are in the direction of their motion. As a result, no side loads are imposed on the piston and displacer seals, which accounts for the favorable endurance characteristics of the linear Stirling refrigerator.

3. PRESSURE VARIATIONS IN A STIRLING REFRIGERATOR

The design, and hence the understanding, of this type of Stirling refrigerator requires that the pressure variations which occur in its working volume be well formulated. A theoretical expression for these pressures variations is given in References 2 and 3, and is not discussed in this report.

The pressure variations which occur in the refrigerator's working volumes are induced by:

- Motion of the piston. Its position determines the total volume.
- Motion of the displacer. Its position determines the amount of gas, at a given time, in the compression (i.e., cold) space and the expansion (i.e., warm) space.
- Gas flow induced by motion of the piston. This flow gives rise to pressure differences in the working volumes.
- Gas flow induced by motion of the displacer. The effects of this motion on the pressure in the refrigerator are similar in nature to those caused by the motion of the piston. Specifically:

The motion of the piston, with the displacer in a fixed position, induces a pressure p as given below:

$$p = p_m + \frac{p_m S_p}{V_o B} y = p_m + C_y y \qquad (1)$$

where,

p_m = average cycle pressure

S_p = piston surface area

y = piston position

V_o = maximum expansion volume

$B = \sum_i \frac{V_i \tau_i}{V_o}, \quad \tau_i = \frac{T_c}{T_i}$

V_i = volume of element i

T_c = temperature compression space

T_i = temperature of element i

With the piston in a fixed position and the displacer reciprocating, pressure p is given by:

$$p = p_m + \frac{p_m S_d (\tau - 1) x}{V_o + \ldots} = p_m + C_x x \qquad (2)$$

where, S_d = displacer cross-sectional area, $\tau = T_c/T_e$ the temperature ratio between the two varying spaces, and x = displacer position.

The change in pressure caused by the motion of the displacer is of course induced by the working gas shuttling between a cold and a warm volume.

The pressure in the cycle, with no flow losses taken into consideration, is given by:

$$p = p_m + C_y y + C_x x \qquad (3)$$

where:

- x = displacer position
- y = position position
- C_x = constant related to pressure variation induced by position of displacer
- C_y = constant related to pressure variation induced by position of piston.

The flow losses of course have to be considered, since they affect the pressure in the various spaces of the refrigerator. The pressure differences across a resistive element (such as a regenerator matrix for instance) which is induced by the gas flow (assumed to be laminar) is given by

$$\Delta p = \frac{c_1 \eta}{\rho v d_h} \frac{l}{d_h} \frac{1}{2} \rho v^2 = c.v \qquad (4)$$

where:

- l = length of resistance
- d_h = characteristic diameter
- ρ = gas density
- v = gas velocity
- η = viscosity
- c and c_1 are constants.

It should be noted that the velocity of the working gas at a point in the refrigerator is the vectorial sum of two velocities which are proportional to the velocity $\dot{y}$ of the piston and the velocity $\dot{x}$ of the displacer. Also, the pressure difference across a resistive element can be translated to pressure changes on its two sides.

The foregoing analysis and discussion leads to expressions giving the pressure variations (p_c) in the compression volume and that (p_e) in the expansion volume.

$$p_c = p_m + C_y y + C_x x + C_{pc}\dot{y} + C_{dc}\dot{x}, \tag{5}$$

$$p_e = p_m + C_y y + C_x x + C_{pe}\dot{y} + C_{de}\dot{x} \tag{6}$$

and to the difference

$$p_e - p_c = (C_{pe}-C_{pc})\dot{y}+(C_{de}-C_{dc})\dot{x}=C_{pp}\dot{y}+C_{dd}\dot{x} \tag{7}$$

where: C_p = a constant related to the flow loss induced by the piston velocity

C_d = a constant related to the flow loss induced by the displacer velcoity

c and e = subscripts referring to the compression and expansion sides, respectively

$C_{pp} = C_{pe} - C_{pc}$

$C_{dd} = C_{de} - C_{dc}$

$\dot{x}$ = displacer velocity

$\dot{y}$ = piston velocity

Equations (5), (6) and (7) are valid only if constants C_y, C_x, C_{dd} and C_{pp} are independent of x, y, $\dot{x}$, and $\dot{y}$, which is not quite the case. Consequently, these three equations are approximations only. As shown in Figures 2, 3 and 4, the approximations are acceptable.

It should be noted that in addition to the factors which induce pressure variations discussed thus far, there are several other second-order contributing factors, viz., leakage past the piston, temperature variations due to heat transfer to walls and due to imperfect mixing, changes in the average temperatures in the heat exchangers and in the varying volumes due to changes in loading, and several others. In addition, the flow is not laminar throughout the refrigerator. Therefore, flow resistances are not linearly dependent on gas velocities, as assumed in Equation (4).

The variation of constants C_x, C_y, C_{dd} and C_{pp} was investigated with the aid of the Philips Stirling Computer Program applied to the MMC-80 refrigerator, a commercially available unit.

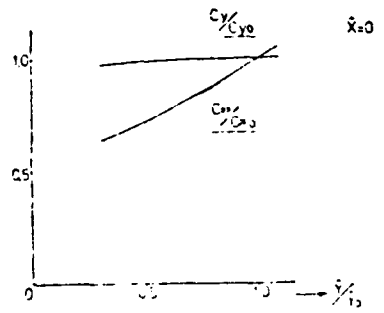

Fig. 2. - Relative variation of C_y and C_{pp} versus relative piston amplitude

Figure 2 shows the variation of C_y and C_{pp} as a function of piston amplitude $\hat{y}$ (with the displacer stationary). As the graph indicates, C_y varies only slightly, most likely due to changes in temperature at different points in the refrigerator. The variation in C_{pp} is more pronounced, due in large part to non-laminar flow.

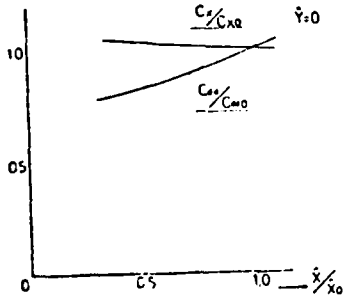

Fig. 3. - Relative variation of C_x and C_{dd} as a function of relative displacer amplitude

Figure 3 shows the variation of C_x and C_{dd} as a function of displacer amplitude $\hat{x}$ (with the piston stationary). As in the previous case, the variation in C_x is comparatively small, and that of C_{dd} is more pronounced.

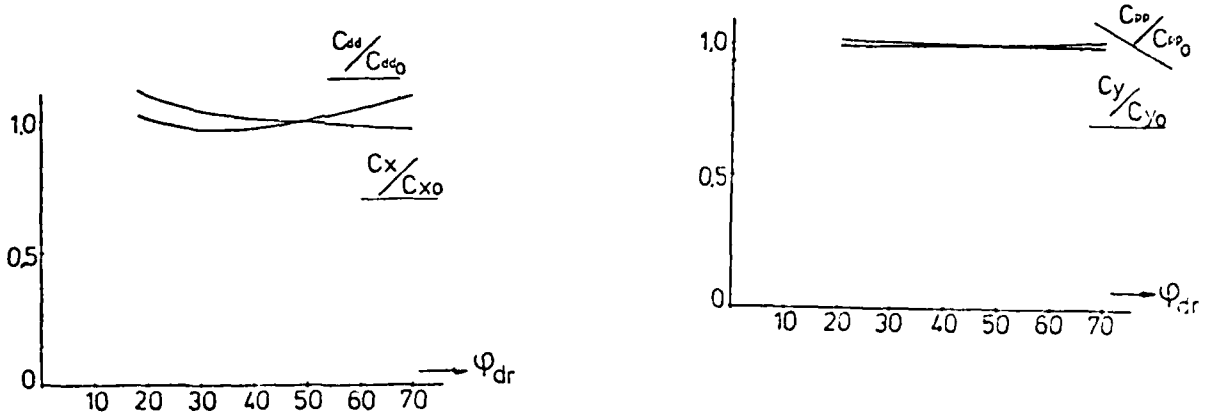

Fig. 4. - Effect of phase shift on the constants C_x, C_{dd}, C_y and C_{pp} with constant piston and displacer amplitude

Figures 4a and 4b show the variations of the four constants as a function of the phase angle between the movements of the piston and the displacer. As the graphs indicate, the variations are relatively small.

4. COLD PRODUCTION AND INPUT POWER

The expressions for the pressure variations which occur in the refrigerator serve in determining its cold production and the power input to it.

The ideal cold production (Q_{eo}) is given by the expression:

$$Q_{eo} = n \oint p \, dV_d = - n \pi C_y \hat{x} \hat{y} S_d \sin \varphi_{dr} \qquad (8)$$

where
$dV_d = S_d dx$ = volume variation of expansion volume
n = number of cycles per second, i.e., speed
$x = \hat{x} \cos \alpha$
$y = \hat{y} \cos (\alpha - \varphi_{dr})$
$\alpha = \omega t$
ω = angular frequency

As Equation (8) indicates, only C_y, reflecting the pressure variations induced by the piston, enters into the expression for the ideal cold production of the refrigerator.

The ideal input power (N_p) is given by the expression:

$$N_p = n \oint p dV_p = n \pi C_x \hat{x} \hat{y} S_p \sin \varphi_{dr}, \qquad (9)$$

where: $dV_p = S_p dy,$

As can be seen in Equation (9), only C_x, or the pressure variations induced by the movement of the displacer, affect the ideal input power to the refrigerator.

From the above equation, two modes of operation can be observed for a positive sin ϕ_{dr}, viz., shaft power is put into or obtained from the system ($C_x > 0$, $C_x < 0$, respectively). More specifically, these two modes are the classical Stirling refrigerator ($\tau > 1$) and Stirling engine ($\tau < 1$) cycles.

5. MOTION OF FREE DISPLACER

The most significant advantage of the concept depicted in Figure 1 is the free motion of the displacer, viz., no mechanical means are required to reciprocate it in the desired phase relationship to the piston. However, to insure proper motion, a number of parameters have to be judiciously established. Some aspects of displacer parameter interaction are presented in this section.

The equation of motion for the displacer is given by:

$$M_d \ddot{x} + (p_e - p_c) S_d + C_{vd} x = 0 \qquad (10)$$

where, $M_d\ddot{x}$ = acceleration force (M_d is the displacer mass), $(p_e-p_c)S_d$ = driving force on the displacer, and $C_{yd}x$ = spring force (friction is neglected).

Integrating the expressions for the pressure into the above equation yields:

$$M_d\ddot{x} + C_{dd}S_d\dot{x} + C_{vd}x = (-C_{pp})S_d\dot{y}, \ (C_{pp}<0). \qquad (11)$$

which is the equation for a damped oscillator with a driving force, in which the driving force $(- C_{pp}) S_d\dot{y}$ is the result of the piston motion, and the damping force $C_{dd}S_d\dot{x}$ results from the motion of the displacer.

If one sets:

$$y = \hat{y} \cos (\alpha - \phi_{dr}) \qquad \text{and} \qquad (12)$$

$$x = \hat{x} \cos \alpha, \qquad (13)$$

then:

$$M_d(\omega^2-\omega_d^2)\hat{x} \cos\alpha + C_{dd}S_d\hat{x}\,\omega \sin\alpha = (-C_{pp})S_d\omega\hat{y} \sin (\alpha - \varphi_{dr}) \qquad (14)$$

where, $\omega_d^2 = \frac{C_{vd}}{M_d}$

Also,

$$\tan \varphi_{dr} = \frac{M_d(\omega_d^2 - \omega^2)}{C_{dd} S_d \omega} \tag{15}$$

and

$$\dot{x} = C_{pd} \vartheta \cos \varphi_{dr} \tag{16}$$

where

$$C_{pd} = \frac{-C_{pp}}{C_{dd}}$$

If $\omega = \omega_d$, which is the condition where the displacer is tuned to the running frequency, $\phi_{dr} = 0$, and consequently no refrigeration is produced. However, if $\omega_d > \omega$, then $\phi_{dr} > 0$, and the unit will operate as a refrigerator.

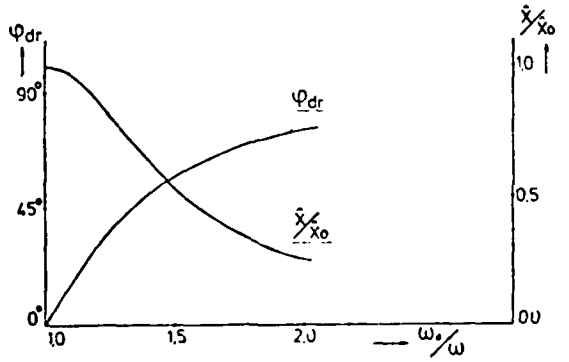

Fig. 5. - Phase shift and relative amplitude of the displacer versus ω_d/ω

In Figure 5, $\dot{x}$ and ϕ_{dr} are given as a function of ω_d/ω. As the graph indicates, when ω_w/ω increases, ϕ_{dr} increases, but $\dot{x}$ decreases.

If equation (16) is integrated into (8),

$$Q_{eo} = -n\pi C_y C_{pd} S_d \vartheta^2 \sin \varphi_{dr} \cos \varphi_{dr} \tag{17}$$

and the optimum, or the maximum amount of refrigeration will occur at $\phi_{dr} = 45°$, or

$$Q_{eo\ max} = \frac{-n\pi C_y S_d C_{pd} \vartheta^2}{2} \tag{18}$$

Then, according to (16)

$$\frac{M_d(\omega_d^2 - \omega^2)}{C_{dd} S_d \omega} = 1 \qquad \text{or} \tag{19}$$

$$C_{vd} = M_d \omega^2 + C_{dd} S_d \omega \tag{20}$$

Introducing a friction force $F_{fr} = F\dot{x}/|\dot{x}|$, Equation (15) becomes

$$\tan \varphi_{dr} = \frac{M_d (\omega_d^2 - \omega^2)}{C_{dd} S_d \omega + 4F/\pi/\hat{x}} \tag{21}$$

and Equation (16) becomes

$$\hat{x} = C_{pd} \hat{y} \cos \varphi_{dr} - \frac{4F/\pi}{C_{dd} S_d \omega} \tag{22}$$

With the introduction of the friction force, the amplitude $\dot{x}$ decreases slightly, causing a corresponding decrease in Q_{eo}, which will now occur at a somewhat smaller value of ϕ_{dr}.

6. MOTION OF THE PISTON

As indicated in Section 1, the piston is driven by a linear electric motor. Its equation of motion is given by:

$$M_p \ddot{y} + (p_c - p_m) S_p + B_g l_v i + C_{vp} y = 0 \tag{23}$$

where

$M_p \ddot{y}$ is the acceleration force (M_p is mass of moving part), $(p_c - p_m)S_p$ the gas force on the piston, $C_{vp} y$ the spring force and $B_g l_v i$ the electromagnetic force. B_g is the magnetic field in the gap, l_v the length of wire present in the gap and i the current through the coil [5]

It should be noted that the friction force was neglected in Equation (23).

The electric current through the motor coils is given by

$$i = \frac{U_o \cos(\beta + \varphi) - U_m}{R_i} = \frac{U_o \cos(\beta + \varphi) - B_g l_v \dot{y}}{R_i} \tag{24}$$

where

$U_o \cos(\beta + \varphi)$ is the voltage of the source ($\beta = \alpha - \varphi_{dr}$ and φ is the fase between voltage and piston movement), U_m is the inductive voltage due to the movement of the coil and thus equal to $B_g l_v \dot{y}$.

When Equation (24) and the expression for the working pressure are integrated in (23),

$$(M_p\omega^2 - S_p C_y - C_{vp})\xi \cos\beta + B_c\omega\xi \sin\beta = S_p C_x \hat{x} \cos(\beta + \varphi_{dr}) - B_u U_o \cos(\beta + \varphi) \tag{25}$$

It should be noted that the above expression does not include the flow losses. Also, the expression includes:

$$y = \xi \cos\beta$$
$$x = \hat{x} \cos(\beta + \varphi_{dr})$$

and $B_c = \frac{(B_g l_v)^2}{R_i}$ and $B_u = \frac{B_g l_v}{R_i}$ have been introduced.

The spring constant for the piston has two components: C_{vp}, the mechanical spring constant, which is relatively small; and $C_y S_p$, the constant for the gas spring. Solving equation (25) with the aid of (21) and (22) gives

$$\tan\varphi = \frac{B_c\omega + S_p C_x C_{pd} \sin\varphi_{dr} \cos\varphi_{dr}}{S_p C_x C_{pd} \cos^2\varphi_{dr} - (M_p\omega^2 - C_y S_p - C_{vp})} \tag{26}$$

As the above expression indicates, ϕ is independent of the applied voltage V_o, but strongly dependent on resonant condition. Also,

$$\xi = \frac{B_u U_o \sin\varphi}{B_c\omega + S_p C_x C_{pd} \sin\varphi_{dr} \cos\varphi_{dr}} \tag{27}$$

which indicates that the amplitude of the piston motion is proportional to the applied voltage.

The power delivered to the piston is given by:

$$N_p = \frac{1}{\pi}\int_0^{\pi} F_m \dot{x}\, dt = \frac{\omega\hat{x}}{2}(B_u U_o \sin\varphi - B_c\omega\xi) \tag{28}$$

The electric power input is:

$$N_{el} = \frac{1}{\pi}\int_0^{\pi} U_o \cos(\beta+\varphi) i\, dt = \frac{B_u U_o}{2B_c}(B_u U_o - \omega\xi B_c \sin\varphi) \tag{29}$$

Hence, the efficiency is given by:

$$\eta_e = \frac{N_p}{N_{el}} = \frac{A \sin^2 \varphi}{(1+A)(A+\cos^2\varphi)} \quad \text{with } A = \frac{N_p}{B_c(\omega \ell)^2/2} \tag{30}$$

The maximum efficiency is reached at $\phi = 90°$.

For optimum η_e and Q_{eo}, that is for lowest power input for highest refrigeration,

$$N_p = \frac{C_v S_p + C_{pd} S_p C_x/2}{\omega^2} + C_{vp} \approx \frac{p_m S_p (\frac{C_v}{p_m} + \frac{C_{pd} C_x}{2p_m})}{\omega^2} \tag{31}$$

Thus, if C_{vp} is neglected, the mass of the piston-coil assembly is inversely proportional to ω^2. The speed of the refrigerator is therefore limited by the piston/coil mass, which is, of course, determined by design or constructional considerations. The only manner in which ω can be increased is by increasing $p_m S_p$.

7. EXPERIMENTAL VERIFICATION

The analysis outlined thus far was verified with the aid of the MMC-80 refrigerator, after inclusion of some of the effects previously mentioned in Section 3.

In Figures 6a, 6b and 6c, the displacer amplitude $\hat{x}$, the phase shift ϕ_{dr}, and the cold production Q_e have been plotted against ω_d/ω. In the tests used to derive the plotted data, the piston amplitude $\hat{y}$, the cold-end temperature T_e, and the average pressure p_m were kept constant.

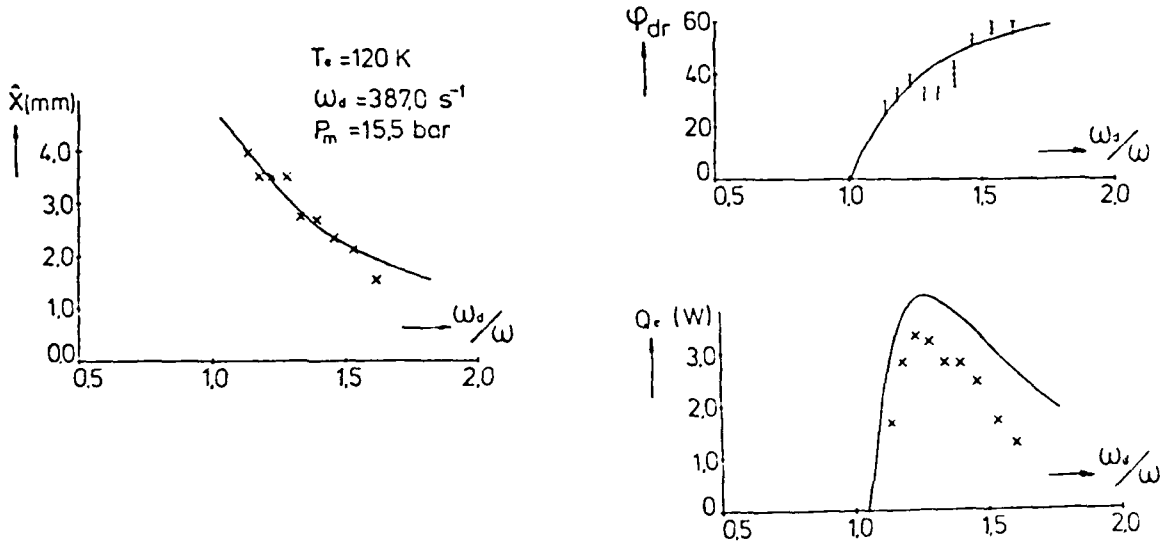

Fig. 6. - Comparison between calculated and experimental results. Displacer amplitude, fase shift and cold production versus ω_d/ω

When a friction loss of F = 0.5 N is assumed, a realistic value in this case, the agreement between theory and practice for $\hat{x}$ and ϕ_{dr} are close. The measured cold production is somewhat lower than that predicted, which is often the case in refrigerators in which the value of the heat losses is comparable to that of the gross cold production.

In Figures 7a, 7b and 7c, the electrical input power N_{el}, the displacer amplitude $\hat{x}$, and the cold production Q_e are plotted against a varying average working pressure P_m, with the piston amplitude $\hat{y}$ kept constant. It should be noted that since the electric input power N_{el} is given by:

$$N_{el} = N_p/\eta_e = B_c(\omega\hat{y})^2/2 \; \frac{(1+A)(A+\cos^2\varphi)}{\sin^2\varphi} \quad , \qquad (32)$$

the above expression will show a minimum at the point where the piston is in resonance. This is confirmed by Figure 7a.

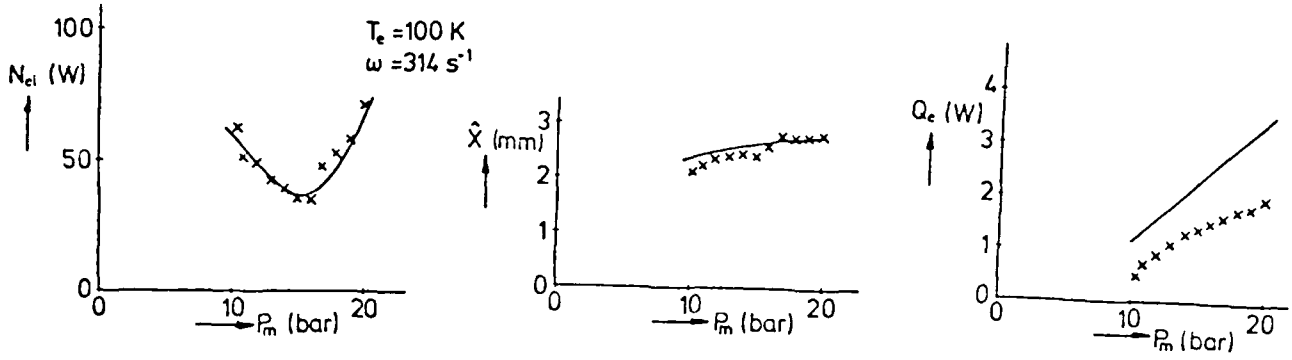

Fig. 7. - Electrical input, displacer amplitude and cold production versus mean pressure with constant ω

8. SUMMARY

A theoretical model was presented for the dynamics of a free-displacer, free-piston refrigerator. The model was verified on a working refrigerator (Model MMC 80) by comparing the theoretically predicted behavior with measured performance.

REFERENCES

1. G.J. Haarhuis, "A Magnetically Driven Stirling Refrigerator", ICEC 7 London, p.422 1978.

2. J.W.L. Köhler and C.O. Jonkers, "Fundamentals of the Gas Refrigerating Machine", Philips Techn. Rev. 16, p.69, 1954.

3. R.J. Meijer, "The Philips Stirling Engine". Ingenieur, vol. 81, May 1969, p. W69, W81.

4. G. Prast and A.K. de Jonge, "A Free Piston Stirling Engine for Small Solar Power Plants". 13th IECEC p.182, 1978.

5. J. Polman, A.K. de Jonge and A. Castelijns, "Free Piston Electrodynamic Gas Compressor". Proc. 1978 Purdue Compressor Technology Conference, Purdue University 1978, p.241.

NOMENCLATURE

p	pressure
T	temperature
τ	temperature ratio
S	surface area
M	mass
V	volume
B	total volume, normalised to T_c and reduced to V_o
x	displacer position
y	piston position
ω	angular frequency
φ	fase shift between piston and applied voltage
φ_{dr}	fase shift between piston and displacer
n	cycles per second
t	time
α	ωt
β	$\alpha - \varphi_{dr}$
f	$1/t$
Q	cold production
N	power
η	efficiency
U_o	amplitude of the applied voltage
U_{in}	inductive voltage due to the movement of the coil
R_i	resistance of the coil
B_g	magnet field in the gap
l_v	length of wire present in the gap
i	electric current
B_c	constant = $(B_g l_v)^2/R_i$
B_u	constant = $(B_g l_v)/R_i$
A	ratio between N_p and $B_c(\omega\varsigma)^2/2$
F_{fr}	friction force acting on the displacer
C_x	constant of pressure variation due to displacer position
C_y	constant of pressure variation due to piston position
C_p	constant of flow loss due to piston velocity
C_d	constant of flow loss due to displacer velocity
C_{pp}	$= C_{pe} - C_{pc}$
C_{dd}	$= C_{de} - C_{dc}$
C_{pd}	$= -C_{pp}/C_{dd}$
C_v	spring constant

Subscripts

m	mean value
c	compression side
e	expansion side
i	volume i
d	displacer
p	piston
0	reference value